Call: H2020-SC5-2014-two-stage

Topic: SC5-01-2014

PRIMAVERA

Grant Agreement 641727

PRocess-based climate sIMulation: AdVances in high resolution modelling and European climate Risk Assessment

Deliverable D*2.5*

Minimal required model resolution

Deliverable Title	*Minimal required model resolution*
Brief Description	Conclusions on the minimum requirements in terms of model resolution for a reliable representation of the North Atlantic, Arctic and Pacific climates, the tropical cyclones and their impact on European climate and on their projected changes in future based on Stream 2 simulations from WP6. This deliverable is distilled from the work that has been done for the stream 2 simulations in WP2 Tasks T2.1-2.3.
WP number	WP2
Lead Beneficiary	*Rein Haarsma, KNMI*
Contributors	Remko Klaver, KNMI Eirini Tsartsali, KNMI Panos Athanasiadis, CMCC Alessio Bellucci, CMCC Daniele Peano, CMCC Enrico Scoccimarro, CMCC Julien Boe, CERFACS Svenya Chripko, CERFACS Rym Msadek, CERFACS Victor Rousseau, CERFACS Emilia Sanchez, CERFACS Ramon Fuentes Franco, SMHI Torben Koenigk, SMHI Jeremy Grist, NERC LP Caron, BSC Eduardo Moreno-Chamarro, BSC Malcolm Roberts, Laura Jackson, Met Office

	Steve Delhaye, UCLouvain Gaëlle Gilson UCLouvain Dmitry Sein, AWI Alex Baker, UREAD Reinhard Schiemann, UREAD Benoit Vanniere, UREAD Federico Fabiano, CNR Virna Meccia, CNR Hannah Christensen, OXF Kristian Strømmen, OXF		
Creation Date Version Number Version Date			
Deliverable Due Date Actual Delivery Date	June 2020 22 July 2020		
Nature of the Deliverable	R	*R - Report*	
		P - Prototype	
		D - Demonstrator	
		O - Other	
Dissemination Level/ Audience	PU	*PU - Public*	
		PP - Restricted to other programme participants, including the Commission services	
		RE - Restricted to a group specified by the consortium, including the Commission services	
		CO - Confidential, only for members of the consortium, including the Commission services	

Version	**Date**	**Modified by**	**Comments**

Table of Contents

1. Executive Summary

This report is a summary of the research performed in Tasks T2.1-3. These Tasks focused on North Atlantic processes (T2.1), Arctic processes (T2.2) and tropical cyclones and their extra-tropical transition (T2.3). The minimal resolution required for a reliable representation of those processes are discussed in detail in this report.

First an important notion needs to be made about resolution. The nominal resolution of models, expressed in grid point distance, is different from the effective resolution, which is the resolution where dynamic processes are not any more affected by the model resolution. This is determined by the shape of the kinetic energy spectrum. The effective resolution is computed for the PRIMAVERA models and is about 2-3 times coarser than the nominal resolution.

For the North Atlantic processes (T2.1), the results indicate that eddy-permitting resolution is required for a reliable representation of North Atlantic Ocean processes, dynamics and air–sea interactions. The added value of eddy-rich simulation could not be clearly evaluated, but the available results warrant further investigation. For the atmosphere, increasing resolution has clearly beneficial impacts for certain aspects, but there are clearly features that appear to be insensitive and do not show improvement. We speculate that parameterizations are in these cases the limiting factor.

For the Arctic processes (T2.2) a finer oceanic resolution generally results in an improvement of the representation of Arctic processes and phenomena, like Arctic sea ice area and volume, Arctic ocean circulation, Atlantic Ocean heat transport and freshwater content. These results are broadly consistent with those obtained for the North Atlantic. Likewise, the results for enhanced atmospheric resolution are also mixed for the Arctic.

For the tropical cyclones and their extra-tropical transition (T2.3), the models show a wide variety of behaviour, with some models in the 20-50 km atmospheric resolution range able to represent observed tropical cyclone frequency, spatial distribution and even intensities. Some characteristics of tropical cyclones are clearly sensitive to resolution (number of storms, maximum surface wind speed), while others are less so (total precipitation of intense cyclones; IKE) and the strongest differences in TC-related characteristics are typically related to the increase in the number of cyclones with resolution.

Summarizing, depending on the processes it is either the oceanic or the atmospheric resolution that mostly affects how they are simulated. Eddy permitting ocean resolution (~0.25 degree) appears in many cases a requirement for a reliable representation. For small scale atmospheric processes like tropical cyclones the results indicate a minimal nominal resolution of 25-50 km for correctly simulating the observed characteristics. For large scale atmospheric phenomena, like blockings, the impact of atmospheric resolution is less clear although generally a positive impact can be discerned.

Because the high-resolution versions of the PRIMAVERA models are not separately tuned, the positive impact of resolution could be masked. It is possible that the tuning of the standard resolution versions compensated for the unresolved processes and that therefore enhancing the resolution deteriorates the simulations. This should be explored in future research.

2. Project Objectives

With this deliverable, the project has contributed to the achievement of the following objectives (DOA, Part B Section 1.1) WP numbers are in brackets:

No.	Objective	Yes	No
A	To develop a new generation of global high-resolution climate models. *(3, 4, 6)*		X
B	To develop new strategies and tools for evaluating global high-resolution climate models at a process level, and for quantifying the uncertainties in the predictions of regional climate. *(1, 2, 5, 9, 10)*	X	
C	To provide new high-resolution protocols and flagship simulations for the World Climate Research Programme (WCRP)'s Coupled Model Intercomparison Project (CMIP6) project, to inform the Intergovernmental Panel on Climate Change (IPCC) assessments and in support of emerging Climate Services. *(4, 6, 9)*		X
D	To explore the scientific and technological frontiers of capability in global climate modelling to provide guidance for the development of future generations of prediction systems, global climate and Earth System models (informing post-CMIP6 and beyond). *(3, 4)*	X	
E	To advance understanding of past and future, natural and anthropogenic, drivers of variability and changes in European climate, including high impact events, by exploiting new capabilities in high-resolution global climate modelling. *(1, 2, 5)*	X	
F	To produce new, more robust and trustworthy projections of European climate for the next few decades based on improved global models and advances in process understanding. *(2, 3, 5, 6, 10)*	X	
G	To engage with targeted end-user groups in key European economic sectors to strengthen their competitiveness, growth, resilience and ability by exploiting new scientific progress. *(10, 11)*		X
H	To establish cooperation between science and policy actions at European and international level, to support the development of effective climate change policies, optimize public decision making and increase capability to manage climate risks. *(5, 8, 10)*		X

3. Detailed Report

Outline of Deliverable D2.5

Because D2.5 is distilled from Task T2.1-3 of DoW performed on the stream 2 simulations, the conclusions that emerge from each of those tasks will be discussed separately. These three individual conclusions will be synthesized to the general conclusion of D2.5. The conclusions of each of the three tasks is supported by the work done by the partners of PRIMAVERA. The relevant work of the PRIMAVERA partners supporting the conclusions distilled from each task will be presented separately and in the general conclusions a reference to these individual contributions will be made.

A reminder of the Tasks T2.1-3:

T2.1 [M1-M48] North Atlantic climate system processes (Lead: KNMI. Participants: SMHI, BSC, CMCC, ECMWF, MET OFFICE, UREAD, CNR, UOXF, MPG, CERFACS, NERC, AWI)

Focus will be on the representation of the North Atlanticocean processes, dynamics and air-sea interactions, and atmosphere dynamics in the North Atlantic/European region. Processes will include ocean mixing, mid-latitude jets and blocking, eddy fluxes of heat, momentum and vorticity, and their combined effect on moisture and heat transports towards Europe, including the occurrence of extreme events such as droughts, heat waves and flooding.

T2.2 [M1-M48] Arctic processes (Lead: UCL. Participants: SMHI, BSC, CMCC, ECMWF, CNR,MPG, CERFACS, NERC, AWI)

Assess the added value of a resolution increase on Arctic sea ice processes including ice concentration, thickness and transport, and ocean-sea ice interactions such as ocean circulation and heat transports and the role of sea ice processes (e.g. melting and freezing) on ocean deep water formation and the AMOC.

T2.3 [M13-M48] Tropical cyclones and their transition to the extra-tropics (Lead: CMCC. Participants: ECMWF, MET OFFICE, UREAD, KNMI, MPG)

Evaluate the benefits of high resolution on the representation of tropical cyclones (including formation and evolution), and their extra-tropical transition and impact on European climate, including associated heat and moisture transports and potential changes in the near future.

Stream2 simulations

In contrast to the DoW stream 2 not only consists of simulations with improvements in the model formulation, but also an enlargement of the stream 1 ensemble size. After finishing the stream 1 simulations it was recognized that natural variability often hampers conclusions about the added value of enhanced resolution. In addition the computing facilities of the centres had improved, allowing to perform more simulations. The results described below are therefore partly based on a larger ensemble of stream 1 simulations and the original designed stream 2 simulations with new model formulations.

3.1 Task T2.1

Summary

Model resolution is usually expressed in nominal grid point distance. However, for correctly representing spatial structures in the atmosphere and ocean at least a few grid points are required. This results in a coarser effective resolution. For the atmosphere the effective resolution of the stream 1 and 2 simulations is computed based on the shape of the kinetic energy spectrum. The effective resolution appears to be 2.7 to 4.8 times lower than the nominal resolution depending on the model (KNMI). For the ocean this is not yet computed, but a similar scaling is hypothesized.

Many aspects of the North Atlantic, Arctic and Pacific climate system processes, ocean processes, dynamics and air-sea interactions, and atmosphere dynamics in the North Atlantic/European region, as outlined in Task2.1, have been analysed and the impact of resolution of the representation of those processes by the stream 1 and 2 models is investigated. A short summary of the research of each of the individual partners of PRIMAVERA is given below this summary.

A definitive answer on the minimum requirements of model resolution for a reliable presentation cannot be distilled from the PRIMAVERA studies. However, the beneficial impact of enhanced resolution emerges in many studies, although also well-known biases that hamper the climate modelling community already for decades, still remain.

In the ocean the increase from 1 degree to 0.25 degree resolution, which marks the jump from eddy parameterized to eddy permitting resolution, allows for a crucial improvement of oceanic process and features, and the processes governing the ocean atmosphere interaction, with a beneficial impact of the atmospheric circulation. This is outlined in numerous studies of the individual PRIMAVERA partners below. The positive impact of the switch from eddy-parameterized to eddy-permitting resolution can be discerned for deep convection in the Labrador Sea and the strength of the Atlantic Meridional Overturning Circulation (AMOC) (SMHI, Met. Office), the representation of the Gulf Stream and its interaction with the atmosphere with implications for the position and strength of the storm tracks (CMCC, KNMI) and the simulation of the North Atlantic subtropical and subpolar gyres (CNR). Apart from a stronger AMOC, eddy-permitting models also simulate a stronger decline in a warmer climate with potential implication for European climate (Met. Office). The improvement of processes by enhancing the ocean resolution from eddy-parameterized to eddy-permitting resolution also shows a clear reduction in biases over the North Atlantic (CMCC).

A few simulations have been made at eddy-rich resolution of 1/12 degree. Clear differences between eddy-permitting simulations are observed in particular over the Gulf Stream region, but a clear improvement of the representation of the processes could not be seen (NERC, KNMI). This might be caused by the still too coarse atmosphere resolution (~25km) (KNMI). In one study, differences in the deep convection in the Labrador Sea compared with eddy-permitting models could not be observed (SMHI), whereas in another study there is a shift in deep convection location from eddy-parameterized (Labrador Sea) to eddy-rich (Denmark overflow) resolution (MPI). A strong positive precipitation signal over Western Europe is observed in a future winter climate in an eddy-rich simulation (BSC). Despite these challenging and interesting results, due to the very small number of simulations and models, firm conclusions cannot yet be made with respect to eddy-rich simulations.

Increasing atmosphere resolution from 100 to 20 km shows a positive impact on the blocking frequency over the Atlantic and the Pacific although no improvement in the duration of blocking events is found (UREAD). Increasing atmosphere resolution also reduces the bias over the Gulf Stream, but this is most effective when the ocean resolution is eddy-resolving (AWI).

Models show a general underestimation of the variance ratio of weather regimes, meaning that the simulated regimes are less evident than in the observations. Increase in atmospheric resolution improves the variance ratio for most models (CNR).

In AMIP simulations no impact of atmosphere resolution on the vertical mixing mechanism (VMM) and pressure adjustment mechanism (PAM[1]) was discerned (CERFACS). In addition, neither a higher resolution nor the realistic representation of the evolution of sea surface temperature and sea-ice leads to a better simulation of sea level pressure trends (CERFACS)

Processes on subgrid scale have to be parameterized. Adding stochastic forcing might be a way to improve the representation of those subgrid scale processes, and for certain aspects of the climate this might be a cost-effective alternative to the increase of model resolution. The inclusion of stochastic sea-ice and ocean schemes has revealed a positive impact on links between Arctic sea-ice and European climate variability, thereby opening alternative ways for improving models (UOXF).

In summary, we can conclude that an eddy-permitting resolution is required for a reliable representation of North Atlantic Ocean processes, dynamics and air–sea interactions. The added value of eddy-rich simulation could not be clearly evaluated, but the available results warrant further investigation.

For the atmosphere, increasing resolution has clearly beneficial impacts for certain aspects, but there are clearly features that appear to be insensitive and do not show improvement. We speculate that parameterizations are in these cases the limiting factor.

KNMI

The Gulf stream region, with sharp fronts and large eddy activity is an area with strong ocean-atmosphere interactions. It is also a source region for baroclinic instability shaping the strength and position of the storm tracks that affect the climate of Europe. Correctly simulating ocean-atmosphere interaction is therefore key for correctly simulating the North Atlantic storm track and European climate (Haarsma et al. 2019).

Using stream 1 simulations we have evaluated the ocean-atmosphere interaction and compared it with reanalyses and available observations. Two mechanisms have been investigated in detail: vertical mixing mechanism (VMM) and pressure adjustment mechanisms (PAM). For VMM a clear dependence on resolution exists with increased ocean-atmosphere coupling and better agreement with reanalysis and observations, for both ocean and atmosphere resolution (Fig. T21.1). Based on the available simulations we conclude that for VMM eddy-permitting ocean resolution and comparable atmosphere resolution are required for a realistic simulation of VMM. For eddy-parameterized ocean resolution the ocean-atmosphere coupling appears to be negligible in the Gulf stream region. The impact of resolution on PAM is less clear. Eddy-parameterized simulations appear to overestimate the coupling. Also, for PAM optimal results are obtained for eddy-permitted ocean resolution and comparable ocean resolution although there is a large spread in the results.

We conclude that eddy-permitting ocean resolution and comparable atmosphere resolution are required for correctly simulating ocean-atmosphere interaction along the Gulf stream. Because most GCMs that are used in the AR5 and AR6 of IPCC are eddy-parameterized models we argue that their representation of the ocean-atmosphere interaction along the Gulf Stream and other western boundary currents is flawed with implications for the dynamics of the storm tracks and the associated climate.

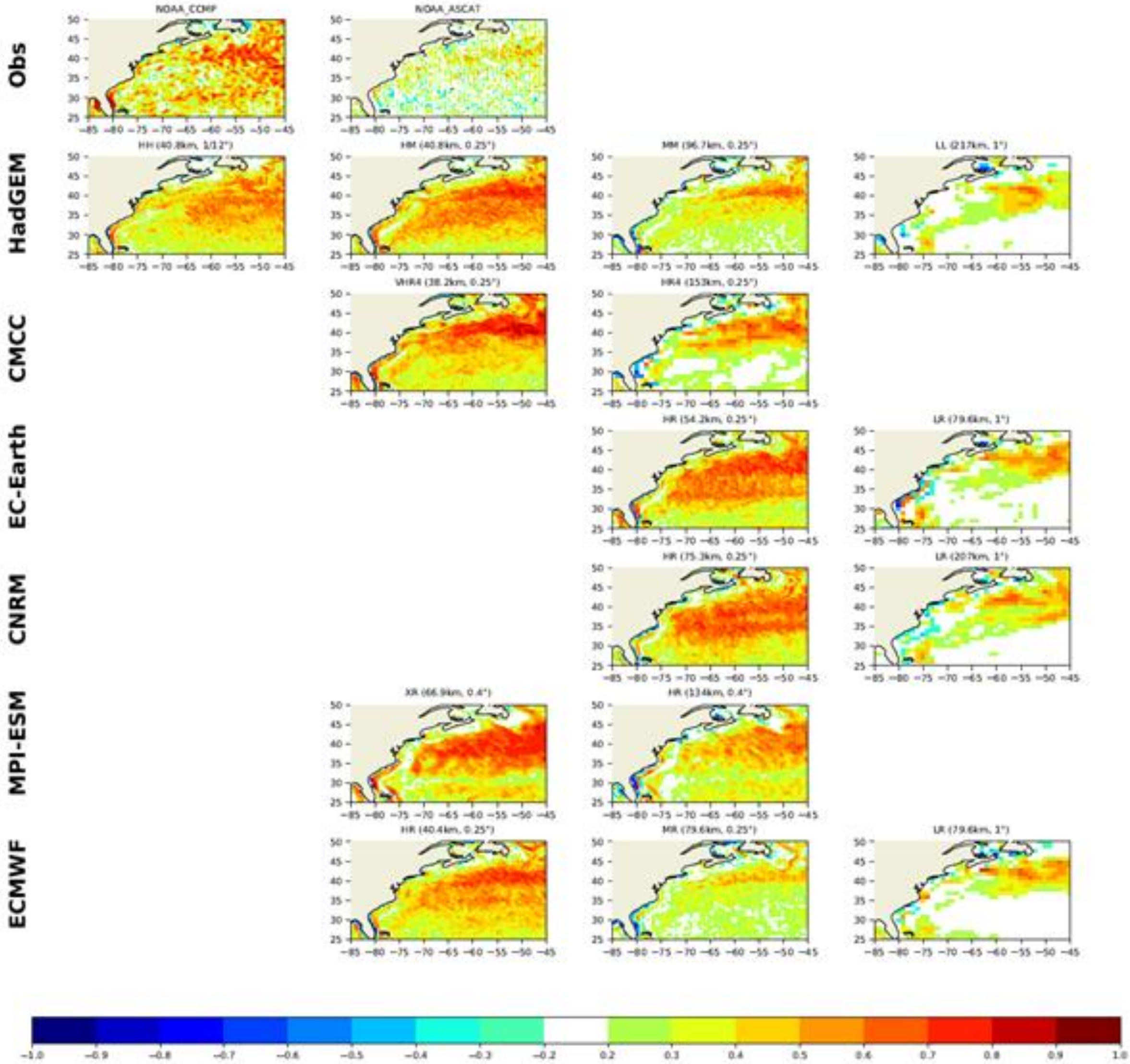

Figure T21.1: *Correlation of time series of spatially high passed wind-stress divergence and downwind SST gradient anomalies. The analysed data are monthly mean values for DJF.*

We have determined the effective resolution of the stream 1 simulations (Fig. T21.2). The highest effective resolution is roughly 200 km (l = 108–110) and is obtained by HadGEM-GC31-HM, CMCC-CM2-VHR4, and ECMWF-IFS-HR. This indicates that the resolution enhancement achieved in these models enables resolving the synoptic scales that are relevant for the dynamics of weather events. The length scale of the effective resolution of the analysed models is between 2.7 and 4.8 times an area weighted mean grid box diagonal.

We find that the ratio of the effective resolution over the grid distance is consistently larger for the high-resolution configurations than for the low resolution counterparts within each of the models. An explanation of this result is outside the scope of this study, but points toward a scale dependency of how nominal resolution is related to effective resolution. Sensitivity studies or the application of the presented diagnostic to a wider range of model resolutions may elucidate the relation between effective resolution and grid distance.

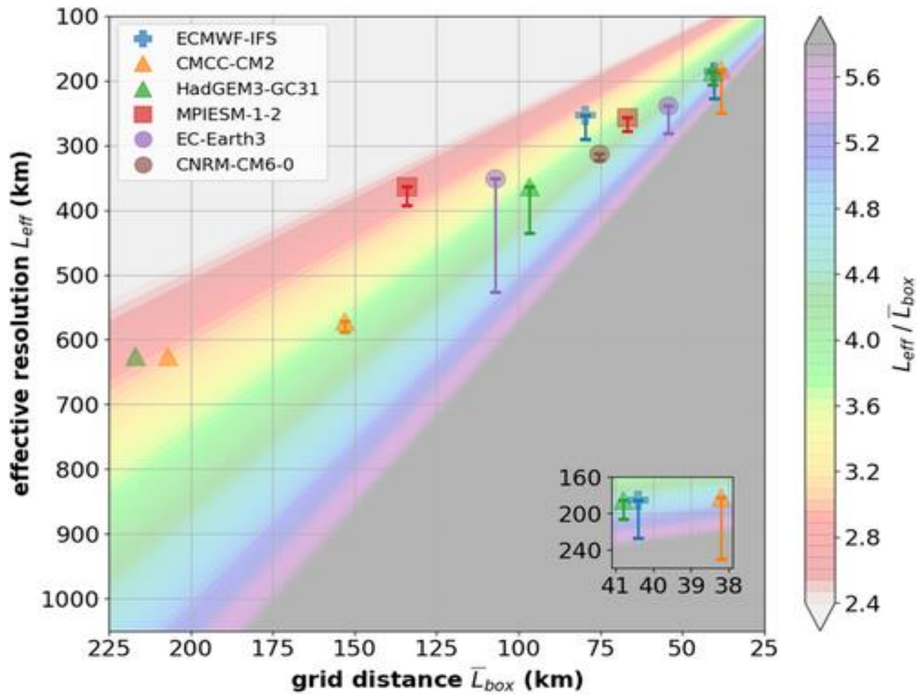

Figure T21.2: *Scatter plot of the effective resolution L_{eff} versus the representative grid box distance L_{box}. Color shading depicts the scaling between effective resolution and representative grid box distance (i.e., y/x). The markers depict the effective resolution, that is, where steepening is diagnosed for two out of the three spectra. The error bar denotes the range of scale at which steepening is diagnosed for one of the three spectra. For the low resolution configurations HadGEM-GC31-LM and CNRM-CM6-0, the markers depict an upper limit of the effective resolution. Error bars are not depicted for these two models. The inlay in the lower right corner provides a zoom of the models ECMWF-IFS-HR, CMCC-CM2-VHR4, and HadGEM-GC31-HM.*

SMHI

Increasing the ocean resolution from around 1 to ¼ degree leads to increased deep convection in the Labrador Sea and reduced convection in the Greenland Sea in the PRIMAVERA historical and control simulations. A further increase to 1/12 degree in the HadGEM3-GC31 model is not further strengthening the convection. Increasing the atmospheric resolution, however, has only little effect on the deep convection.

The vertical density profiles in the convection regions of the Labrador Sea in early winter are more realistic when increasing the ocean resolution (Fig. T21.3). However, despite realistic density distribution, the convection is generally too strong compared to observational data indicating other shortcomings in the models.

Simulated convection in the Labrador Sea is largely governed by the release of heat from the ocean to the atmosphere. Higher resolution models show stronger surface heat fluxes than the standard resolution models in the convection areas, which promotes the stronger convection in the Labrador Sea.

In the Greenland Sea, the connection between high resolution and ocean heat release to the atmosphere is less robust and there is more variation across models in the relation between surface heat fluxes and convection.

The deep convection in the Labrador Sea leads the AMOC at 26°N by a few years in most of the models (not shown) and models with stronger convection show also a stronger AMOC. Thus, higher resolution leads to a stronger AMOC.

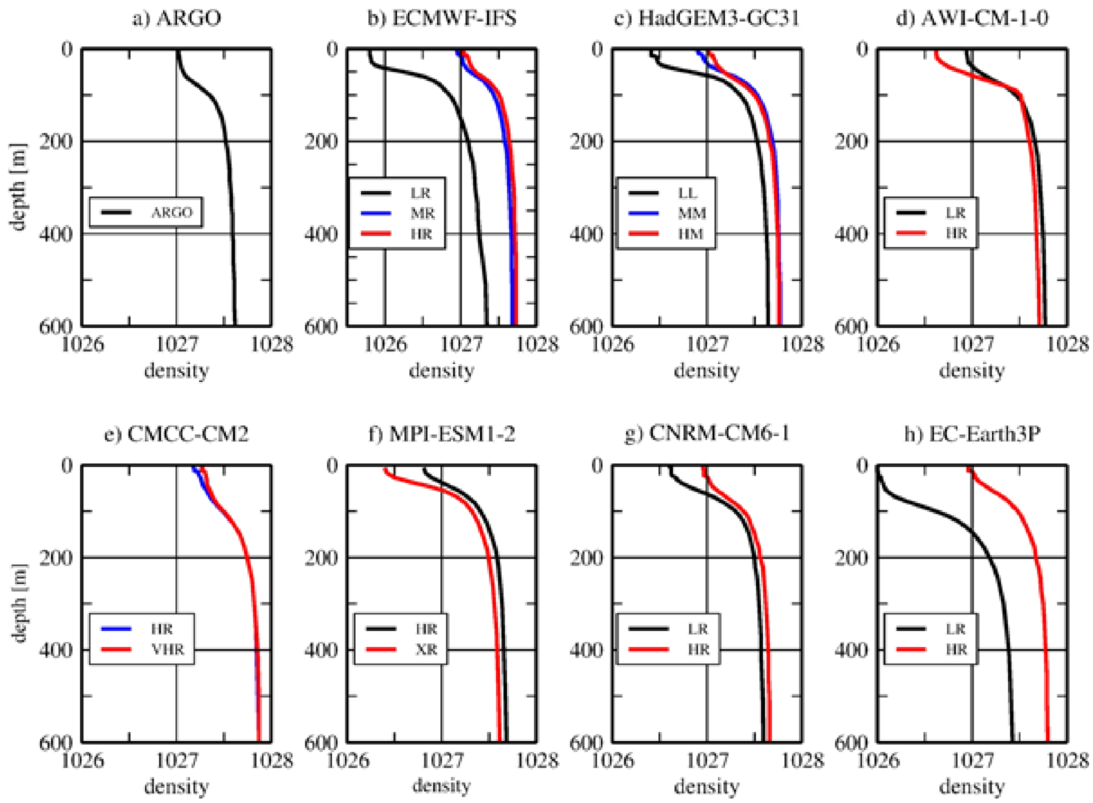

Figure T21.3: *Ocean density in the upper 600m in the Labrador Sea in Argo data (average 2000-2015) and the model simulations.*

BSC

We look at the sensitivity of the projected changes in winter precipitation in Europe to model resolution (Moreno-Chamarro et al., 2020, submitted). We compare changes in winter precipitation between the period 2030–2050 and 1960–1980 in simulations with the coupled climate model HadGEM3-GC31. We find that winter precipitation in Northwestern Europe increases substantially more in the simulation at the highest resolution than at lower resolutions, particularly when using an eddy-rich ocean model. We further find that increased precipitation in NW Europe results from strengthened extratropical cyclones crossing the North Atlantic. These are ultimately fuelled by ocean surface warming in the Gulf Stream, absent at lower resolutions, and show a negligible contribution from changes in atmospheric meridional temperature gradients.

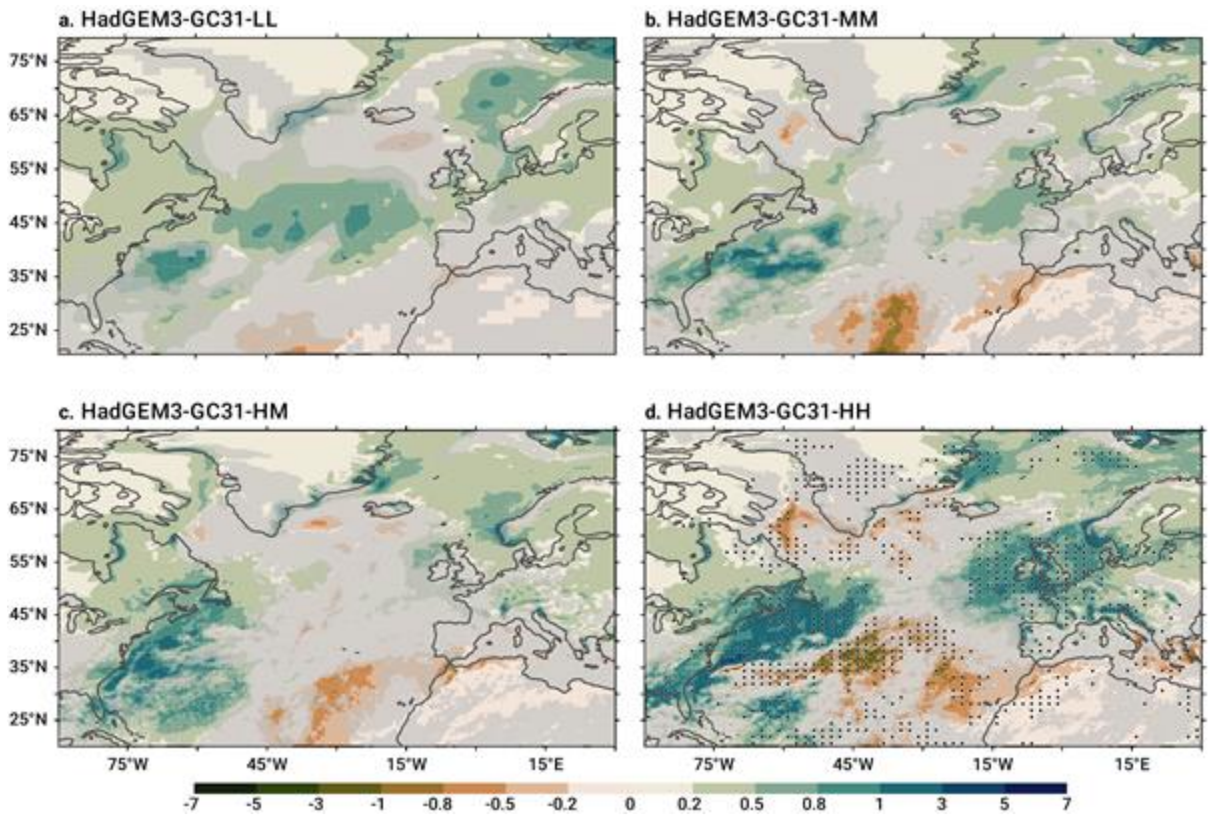

Figure T21.4: *Change in DJF precipitation (mm/day) between 2030–2050 and 1960–1980 in the HadGEM3-GC3.1 model at* ***(a)*** *LL* ***(b)****, MM* ***(c)****, HM, and* ***(d)*** *HH resolutions. Ensemble means are shown for LL, MM, and HM. Gray shading masks non-significant anomalies at the 5% level based on the random occurrence of the signal in the control simulations. Stippling indicates anomalies in HH larger than anomalies in the individual LL, MM, and HM simulations.*

CMCC

(A) Regimes of ocean-atmosphere interactions over the Gulf Stream

This study (Bellucci et al., 2020, submitted) assesses the impact of model resolution on the representation of air-sea interactions over the Gulf Stream region, in the PRIMAVERA ensemble of present-climate (control-1950) simulations. We use the approach outlined in Bishop et al. (2017) to characterize the nature of air-sea interactions, relying on the analysis of the covariance patterns of SST (and SST tendency) and turbulent (latent and sensible) heat fluxes (THF). Based on this approach, the functional shape of the SST-THF covariance reveals whether the ocean-atmosphere co-variability is primarily driven by the atmospheric intrinsic variability (associated with synoptic scale weather) or ocean internal variability (including the effects of mesoscale eddies).

Grid-point covariance patterns of monthly mean SST tendency and THF anomalies in the ±1-month lag interval are shown for models changing both ocean and atmosphere resolution (Fig. T21.5) and models where only the atmospheric resolution is changed (Fig. T21.6). Observational estimates (based on the J-OFURO3 data set) are also shown in each Figure, in the rightmost column. In general, all models show the observed lead-lag relationship between SST and THF along the GS axis, with covariances exhibiting a typical anti-symmetric structure around the zero lag. The anti-symmetric pattern found over the GS is indicative of an ocean-driven regime, consistent with results from 1-dimensional stochastic energy balance models (Wu et al., 2006; Bishop et al., 2017). Comparing low- versus high-resolution configurations in Fig. T21.5, there is a clear improvement in the degree of realism of air-sea covariability associated with models using eddy-permitting (~25 Km) ocean configurations, compared to eddy-parameterised (~100 Km) ocean systems. Increasing the ocean model resolution (moving from “laminar” to “turbulent” oceans) has a beneficial impact on the tilt and overall shape of the GS jet signature, turning from a predominantly zonal to a more realistic SW-NE orientation. On the other hand, models changing only the atmospheric resolution (Fig. 6) exhibit a much weaker sensitivity to enhanced resolution, suggesting that the ocean resolution is the primary responsible for the improved representation of air-sea covariance. Similar considerations hold when looking at the SST-THF covariance patterns (not shown).

These results are consistent with other studies based on the PRIMAVERA multi-model ensemble, analysing different climate-relevant processes (Docquier et al., 2019; Roberts et al., 2020) and corroborate the idea of a critical threshold in the ocean model resolution, roughly placed around the eddy-permitting (~25 km) range, leading to a step-change in the degree of realism of the simulated features.

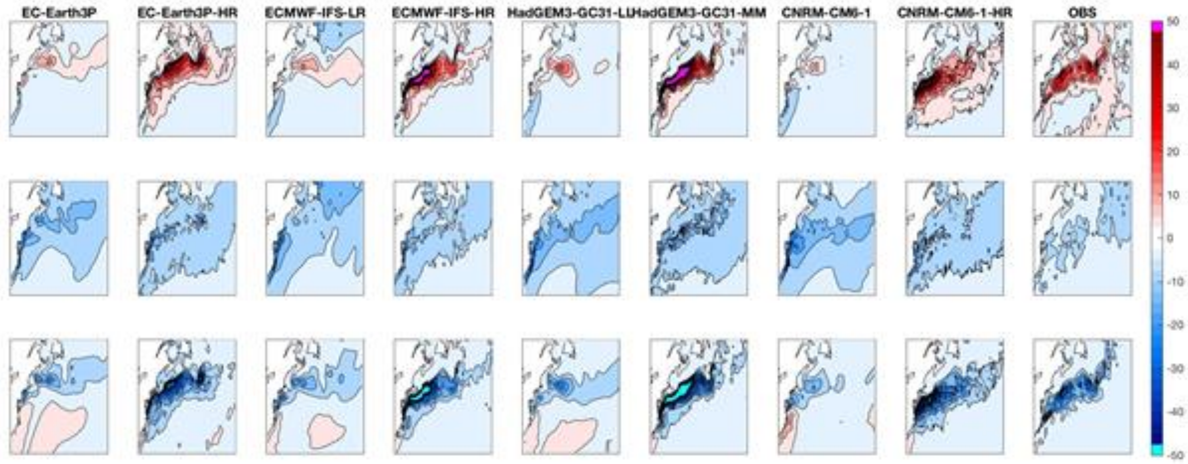

Figure T21.5*: SST tendency-THF covariance patterns in the North Atlantic (ºC W m^{-2} month^{-1}) computed for [-1,0,+1]-month lags (top, mid, bottom row, respectively) for PRIMAVERA models and observations (J-OFURO3 data set). SST tendency leads for negative lags. Models changing both atmospheric and ocean resolution are shown.*

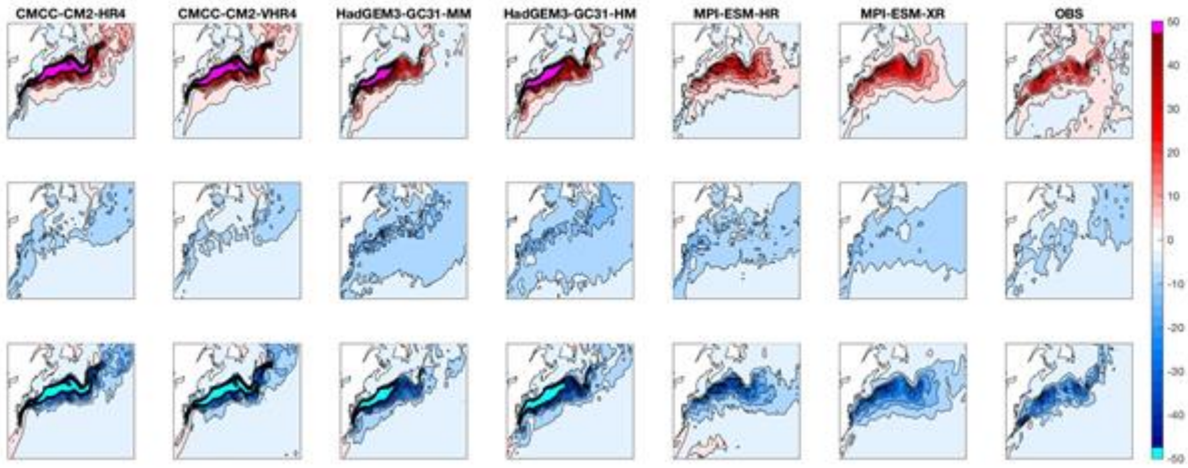

Figure T21.6: *Same as Fig. T21.5 but for models changing only the atmospheric resolution.*

(B) The effect of SST biases and increasing model resolution in the representation of North Atlantic blocking and the jet.

Increasing model resolution (rendering the oceanic model component eddy-permitting and allowing the atmosphere to see and better interact with the ocean mesoscale) has been found to improve models' realism, particularly in the North Atlantic domain. Characteristically, SST biases are found to be reduced at the Gulf

Stream extension and further downstream (Fig. T21.7). Such biases are largely endogenous to the respective oceanic model components but are expected and are known to impact the atmospheric circulation (Keeley et al., 2012; Lee et al., 2018). Significant statistical association (anticorrelation) was found between the magnitude of the SST front meridional gradient at the extended GSE area and the frequency of Greenland blocking in the PRIMAVERA historical Stream-1 coupled simulations (12 models from 6 institutes, results not shown). The impact of the average latitude of the SST front (depended on the Gulf Stream detachment point) was also assessed in this regard. Coming to the role of increasing model resolution, the model biases in Eastern Atlantic blocking and the frequency of occurrence of the north-jet regime (Woollings et al., 2010) are reduced for 5 out of 6 models, comparing High-Res to Low-Res (Fig. T21.8).

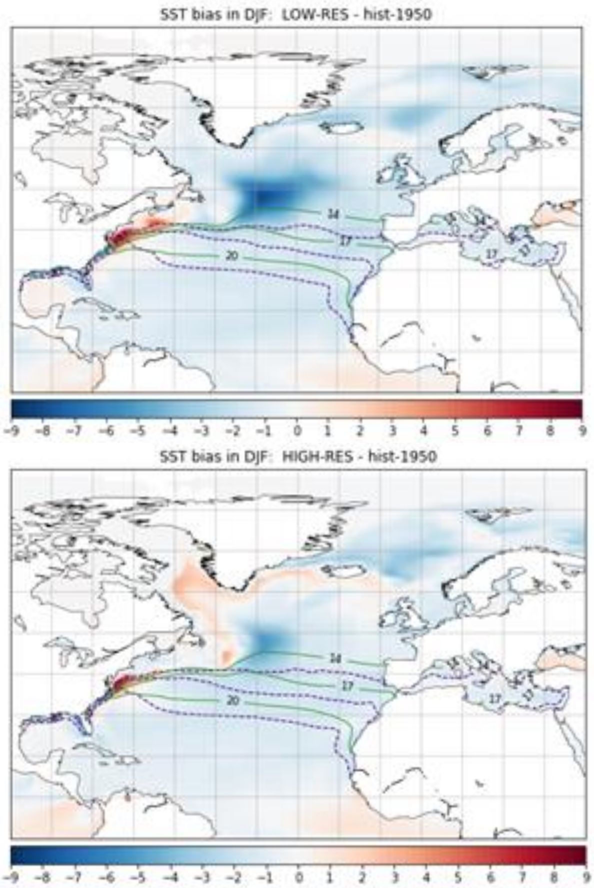

Figure T21.7: *Reduction of wintertime SST biases associated with the increase of model resolution in PRIMAVERA historical coupled simulations (stream-1, hist-1950). The solid green contours correspond to the observed (HadISSTv.2) climatology, while the dashed purple lines are the respective isolines for the multi-model ensemble. The models used to define the two ensembles can be seen in the following figure (Fig. T21.8).*

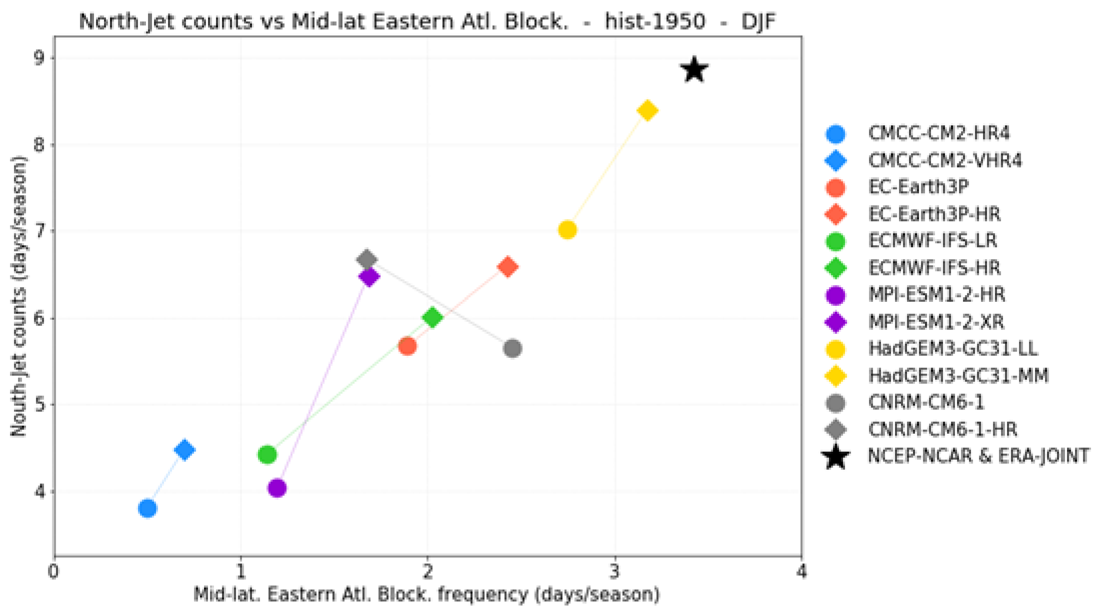

Figure T21.8: *Reduction of wintertime biases in Eastern Atlantic blocking and the North-Jet counts for 5 out of 6 models: diamond (round) markers corresponding to the high-resolution (low-resolution) version of each model.*

MET OFFICE and other partners

The Atlantic Meridional Overturning Circulation (AMOC) is a key component of the ocean circulation in the Atlantic, transporting heat northwards together with warm water, which sinks at higher latitudes and flows southwards at depth. As well as influencing the mean climate, AMOC variability can also imprint on the North Atlantic and European surface climate, as can AMOC future projected change. Grist et al. (2018) looked at model resolution and northward heat transport in early PRIMAVERA model simulations.

Roberts et al. (2020) and Jackson et al. (2020) have assessed the PRIMAVERA-HighResMIP multi-model simulations, looking at both the historic performance and future change. For most models, increased resolution (mainly the ocean) tends to lead to an increase in AMOC strength and northward heat transport, which typically agrees better with the RAPID-MOCHA observational array at 26.5°N. However, in the subpolar gyre many of the higher resolution models have enhanced biases in temperature and salinity, and this contributes to excessive deep mixing in the Labrador Sea, which itself contributes to the stronger AMOC.

In the future, as shown in Fig. T21.9, the models with stronger AMOC in control-1950 (typically the higher resolution models) have a stronger decline in AMOC strength compared to the lower resolutions (bottom right part of the figure). This is a consequence of surface warming reducing the Labrador Sea convection more quickly than in the Nordic Seas, where it can migrate northward to colder conditions. Since the higher resolution models have a larger AMOC component linked to the Labrador Sea, this causes the stronger decline. The stronger decline is also linked to reduced warming in the subpolar gyre, with potential changes over Europe (Haarsma et al. 2015; Grist et al. (submitted); Moreno-Chamarro et al. (submitted)). These processes are stronger in the models using the NEMO ocean, the CESM1.3 model has much weaker future change in their coupled models with 1/10° ocean.

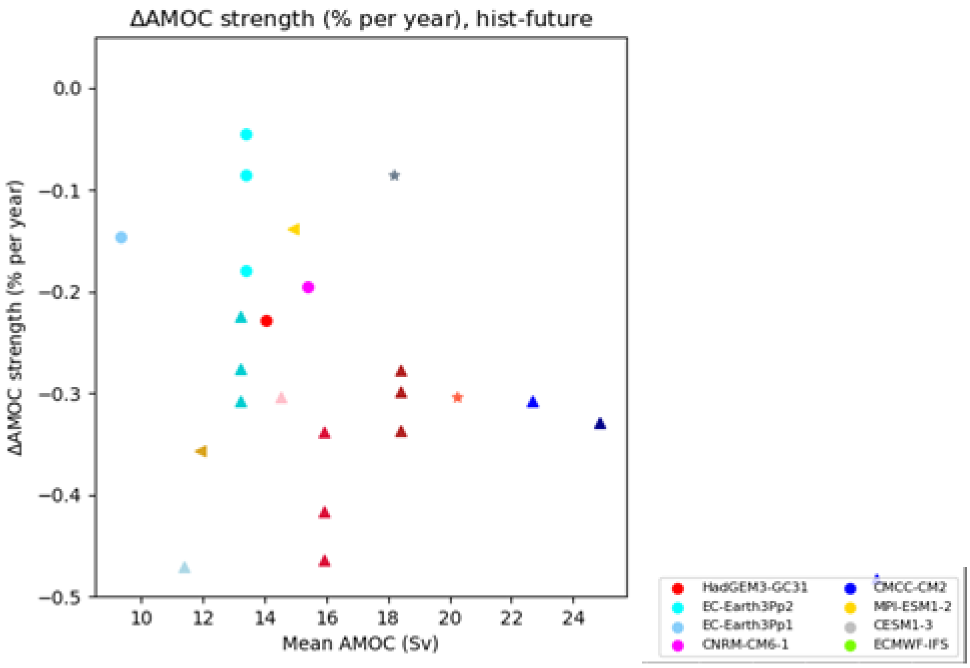

Figure T21.9: *Scatter plot of the mean strength of AMOC in the control-1950 simulations, against the future change in AMOC (expressed as a %per year of the control value) up to 2050 compared to 1950. Circles use 1 degree ocean models, triangles are ¼ degree models and stars are 1/10 or 1/12 degree models.*

UREAD

Global climate models (GCMs) are known to suffer from biases in the simulation of atmospheric blocking, and in this study (Schiemann et al. 2020) we assess how blocking is represented by the latest generation of GCMs. We evaluate (i) how historical CMIP6 simulations perform compared to CMIP5 simulations, and (ii) how horizontal model resolution affects the simulation of blocking in the PRIMAVERA historical simulations. Two blocking indices are used to evaluate the simulated mean blocking frequency and persistence for the Euro-Atlantic and Pacific regions in winter and summer against the corresponding estimates from atmospheric reanalysis data.

Maps of blocking frequency biases are shown in Fig.T21.10, for the CMIP5 and CMIP6 multi-model means, as well as for means of four PRIMAVERA sub-ensembles, which are determined according to whether a model is forced (highresSST-present) or coupled (hist-1950) and to model resolution. A long-standing characteristic blocking bias, namely a widespread underestimation of blocking frequency, can be identified in all the ensembles considered. Closer inspection of Fig. T21.9 reveals an improvement both in the CMIP6 over the CMIP5 models, and in the higher-resolution PRIMAVERA models over the lower-resolution models. These differences are further quantified for the case of winter blocking in the Atlantic-European sector in Figure T21.11. CMIP6 models agree better with the reanalysis estimate in terms of three different metrics (blocking frequency, spatial (pattern) correlation, and root-mean-square error). An improvement can also be seen in the higher-resolution PRIMAVERA simulations, but more so in the pattern correlation, for which 6 of 7 models show an improvement, than for blocking frequency.

In summary, we find robust evidence that CMIP6 models simulate blocking frequency and persistence better than CMIP5 models in the Atlantic and Pacific and during winter and summer. This improvement is sizeable so that, for example, winter blocking frequency in the median CMIP5 model in a large Euro-Atlantic domain is underestimated by 33% using the absolute geopotential height (AGP) blocking index, whereas the same number is 18% for the median CMIP6 model. As for the sensitivity of simulated blocking to resolution, it is found that the resolution increase, from typically 100 km to 20 km grid spacing, in most of the PRIMAVERA models, which are not re-tuned at the higher resolutions, benefits the mean blocking frequency in the Atlantic in winter and summer, and in the Pacific in summer. Simulated blocking persistence, however, is not seen to improve with resolution. Our results are consistent with previous studies (e.g., Woollings et al. 2018) suggesting that resolution is one of a number of interacting factors necessary for an adequate simulation of blocking in GCMs. The improvements reported here hold promise for further reductions in blocking biases as model development continues.

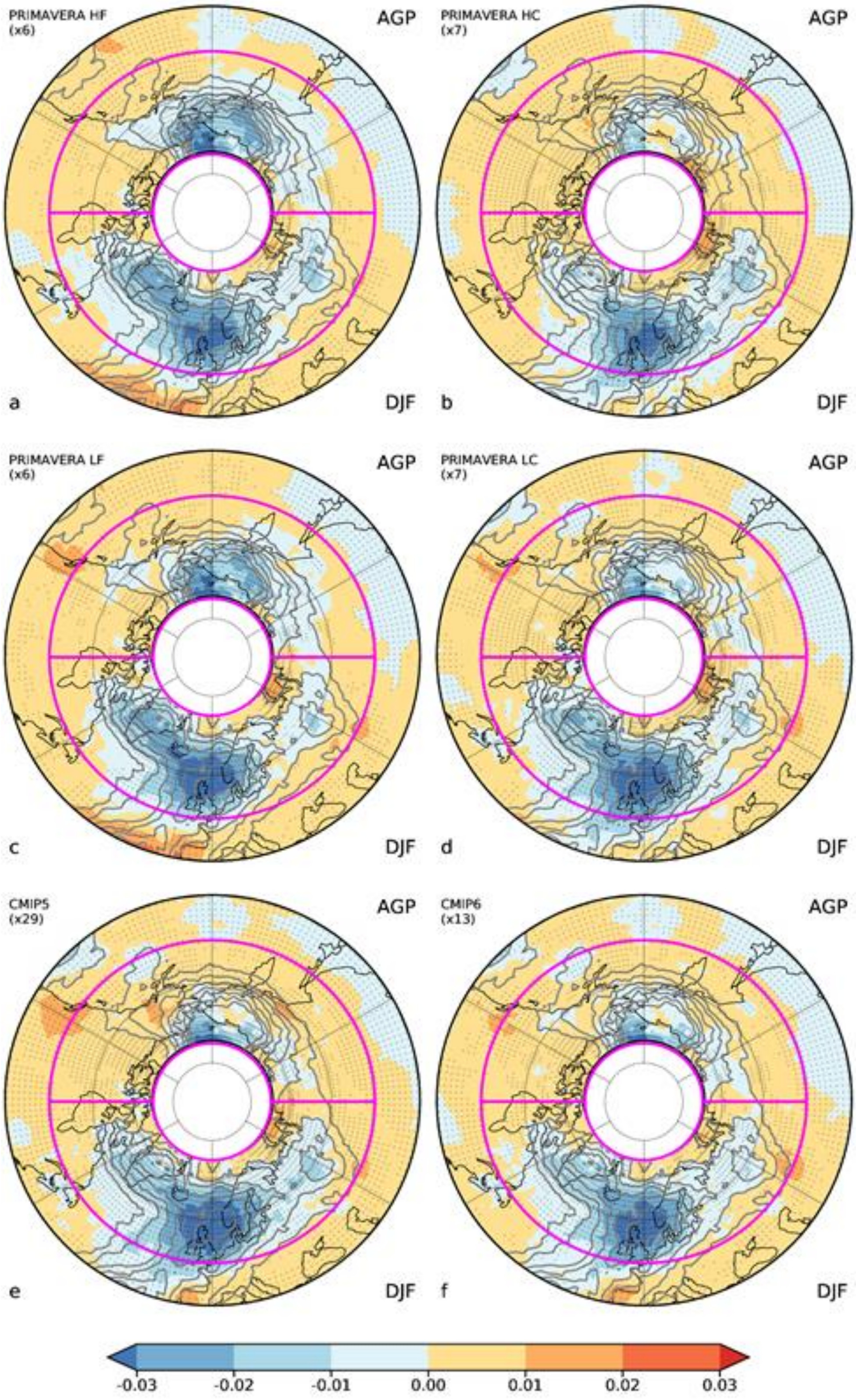

Figure T21.10: *Bias in the frequency of blocked days for the AGP blocking index, boreal winter, and (a) high-resolution forced, (b) high-resolution coupled, (c) low-resolution forced, (d) low-resolution coupled PRIMAVERA simulations, and (e) CMIP5, (f) CMIP6 simulations. Stippling shows agreement on the sign of the bias by at least (a,c) 6 of 6, (b,d) 6 of 7, (e) 19 of 29, and (f) 10 of 13 simulations. Grey contour lines show the reanalysis blocking frequency, at contour intervals of 0.01 start from 0.01. ATL and PAC evaluation domains are shown by magenta lines.*

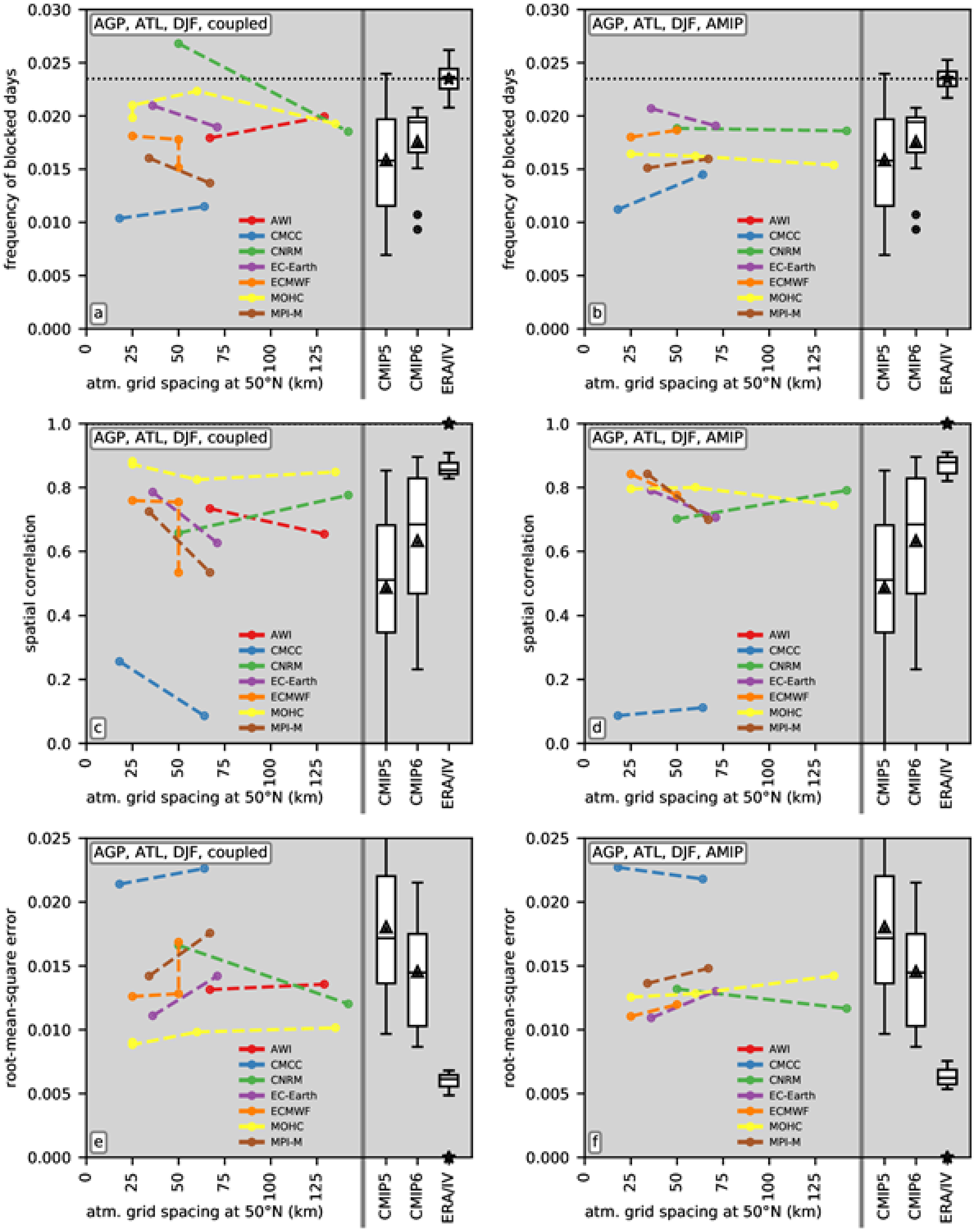

Figure T21.11: *Metrics of blocking performance (a,b - blocking frequency, c,d - spatial correlation, e,f - root-mean-square error) for the AGP index and boreal winter, for the ATL domain (-90-90E, 50-75N). The left-hand side of each panel shows metrics for PRIMAVERA simulations at different grid spacings (resolutions). Boxplots on the right-hand side show distributions of the metric across CMIP5 and CMIP6 simulations in terms of the median, mean (triangle), interquartile range (box, IQR = Q3 - Q1), top whiskers extending to the last datum less than Q3 + 1.5IQR, and analogously for bottom whiskers. The '*' symbol in the column 'ERA/IV' shows the reanalysis estimate and the boxplot is an estimate of the expected agreement given internal variability.*

CNR

Figure T21.12 shows the mean fields of the barotropic stream function in the North Atlantic for the period 1950-2014 as simulated by 5 climate models in two different resolutions (first and second columns) and the difference between them (third column). In all the cases, the climatology clearly displays the subpolar and subtropical gyres (SPG and STG). There are differences in the 2D structure if both the atmosphere and ocean resolutions are increased. In particular, the western tongue of the SPG extends more to the northwest and the intensity of the SPG and the Gulf Stream are stronger with increased resolution (third column of Fig. T21.12). However, it seems that no systematic differences are obtained when the resolution is changed only in the atmosphere, as is the case for CMCC-CM2 and MPI-ESM1-2.

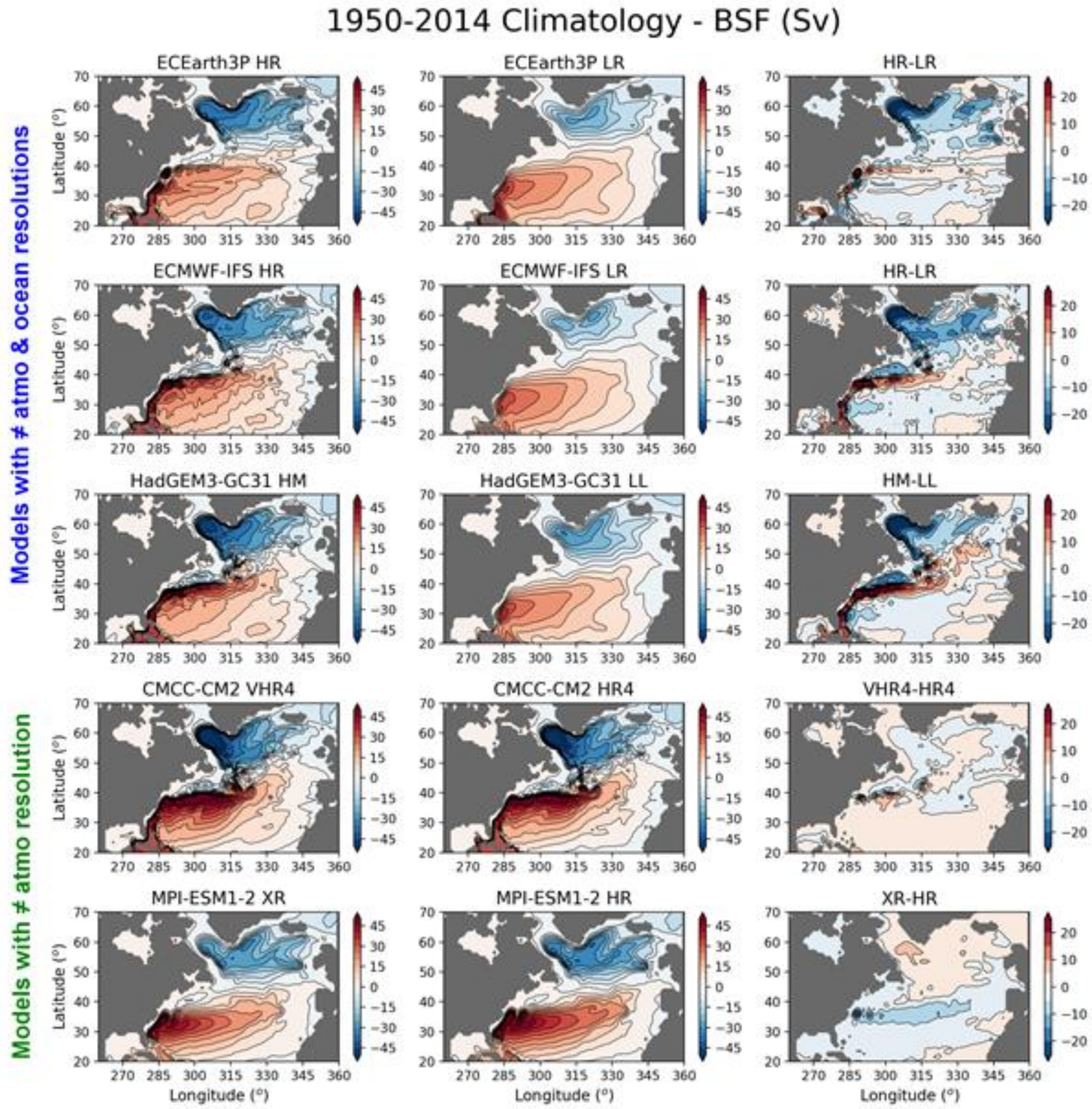

Figure T21.12: *North Atlantic barotropic streamfunction climatology for the period 1950-2014. Results of five climate models in their high (left column) and low (central column) horizontal* *resolutions. The third column shows the difference between both resolutions. One ensemble member for each model configuration is plotted.*

Weather Regimes are large-scale recurrent configurations of the mid-latitude atmospheric dynamics that primarily determine regional climate in Europe. These are obtained through K-means clustering of the daily geopotential field at 500 hPa, in a reduced phase space (for details, see Fabiano et al., under review). A synthetic measure of the model performance in reproducing the observed regime structure is the variance ratio of the clusters: this is the ratio between the average inter-cluster squared distance and the mean intra-cluster variance, and gives a measure of how tightly clustered the data are. Figure T21.13 shows the results for the hist-1950 simulations, compared to the observations. The regime patterns are shown at the top of the Figure for reference.

Models show a general underestimation of the variance ratio, meaning that the simulated regimes are less evident than in the observations. The increase in resolution improves the variance ratio for most models, though some do not show any significant change (CMCC-CM2, MPI-ESM1); in one case (HadGEM3-GC31-HH) the result is worse than the standard resolution. In general, the resolution is playing a role in improving the variance ratio, though the improvement is small and other factors might also be at work. Indeed, a significant correlation has been found between the models' variance ratios and the respective agreement with the observations of the climate mean state over the North Atlantic in terms of the following quantities: geopotential mean field and low frequency variability, mean SSTs, blocking pattern and jet latitude variability. Another factor at play that might be hindering the impact of resolution is model tuning, since many models were only tuned in their standard resolution version.

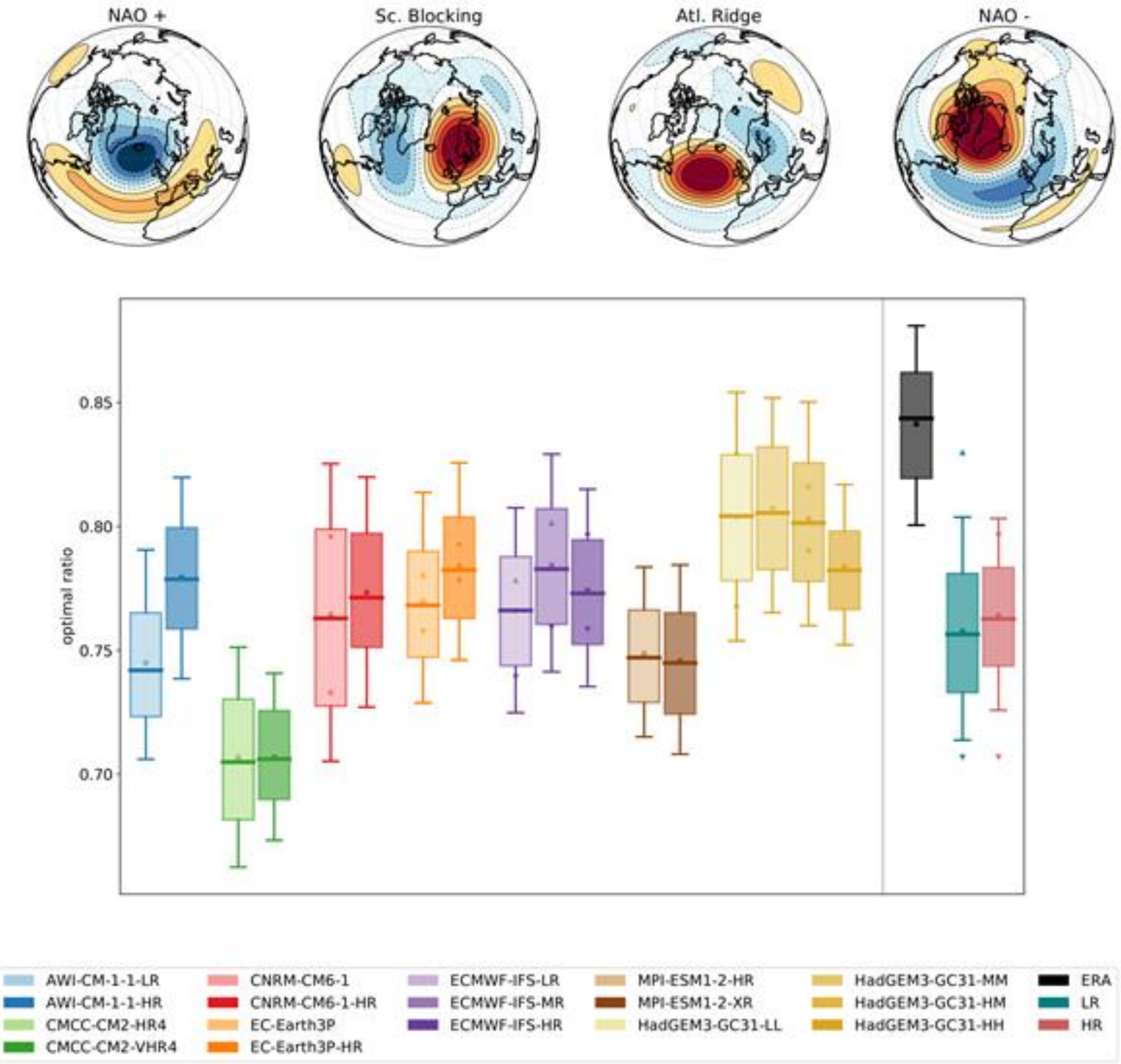

Figure T21.13: *Variance ratio of the Euro-Atlantic Weather Regimes in the hist-1950 coupled simulations. The observed patterns of the 4 regimes are shown at the top for reference. The box plots refer to the distribution of 30-yr bootstraps of each model and show mean (dot), median (horizontal line), first and third quartile (boxes) and 10 and 90 percentiles (bars). At the right of the gray vertical line, three boxes are shown. The first (black box) refers to the ERA 30-year bootstraps. The other two boxes represent average quantities among all the LR and HR models and are calculated as the average of the percentiles and median over all models.*

UOXF

The impact of stochastic sea-ice and ocean schemes on links between Arctic sea-ice and European climate variability:

Multiple studies support the idea that interannual variations in the autumn Arctic sea-ice extent, particularly in the Barents-Kara region, can influence the climate over Europe in the subsequent winter (e.g. Strong et al. 2010, Caian et al. 2017, Wang et al. 2017). The dynamical pathway has both a tropospheric and stratospheric component, with both being initiated by changes in the heat flux from the ocean to the atmosphere as a result of more or less sea-ice cover. In the presence of a positive sea-ice anomaly, a wave-like pattern of temperature anomalies is generated, yielding a cooling in the North Atlantic and a poleward shift of the jet, corresponding to the positive phase of the North Atlantic Oscillation (NAO). The representation of this dynamical pathway in models is therefore crucially linked both to the representation of Arctic sea-ice itself (its mean and month-to-month variance) as well as the subsequent atmospheric response.

We examined the impact of including a stochastic sea-ice and ocean scheme on this teleconnection between Barents-Kara sea-ice and the NAO, using the EC-Earth3P model. These schemes aim to represent uncertainty due to unresolved processes as well as poorly constrained parameters, and were developed by Stephan Juricke (formerly at Oxford) and colleagues (Juricke et al. 2013, 2014, 2017). It was found that the deterministic EC-Earth3P did not capture the observed teleconnection, at either high or low resolution. On the other hand, the simulations with stochasticity included did represent it: see Figure T21.14. We hypothesised that this is due to two complementary reasons. Firstly, the stochastic sea-ice scheme leads to an improved mean and variance of Arctic sea-ice: Figure T21.15 shows this for the mean state. This leads to a more realistic rapid response to the subsequent heat flux anomaly. Secondly, the stochastic ocean-scheme disturbs the influence of tropical Pacific sea-surface temperatures on the NAO, which is overly regular in the deterministic model (not shown). This allows the evolution of the rapid response to propagate more realistically, without being effectively eliminated by a strong tropical signal. It may therefore be beneficial to include a stochastic sea-ice and ocean component.

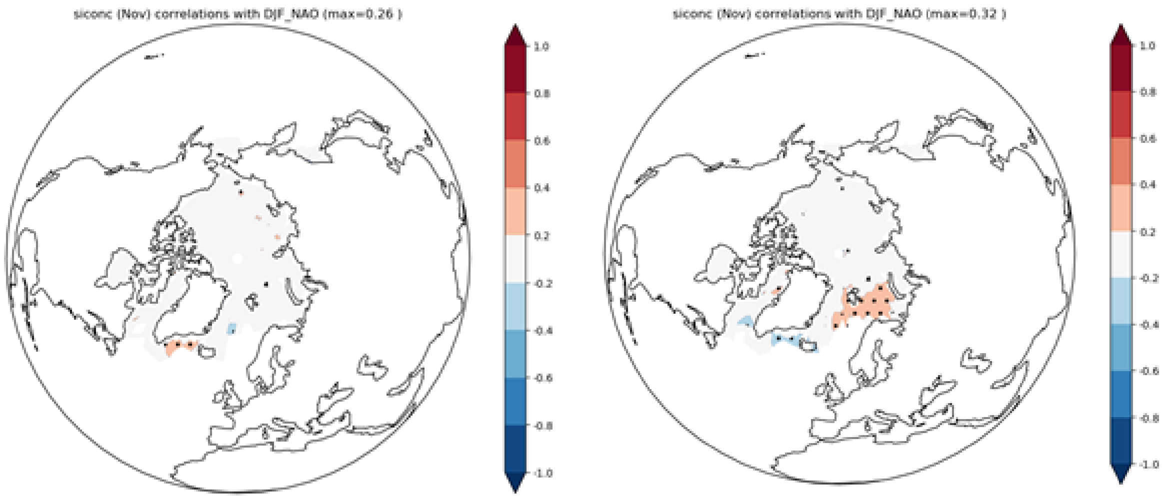

Figure T21.14: *Correlations between detrended sea-ice concentration anomalies in November at individual gridpoints against the subsequent winter NAO index, 1980-2015. Left: deterministic EC-Earth3P. Right: stochastic EC-Earth3P.*

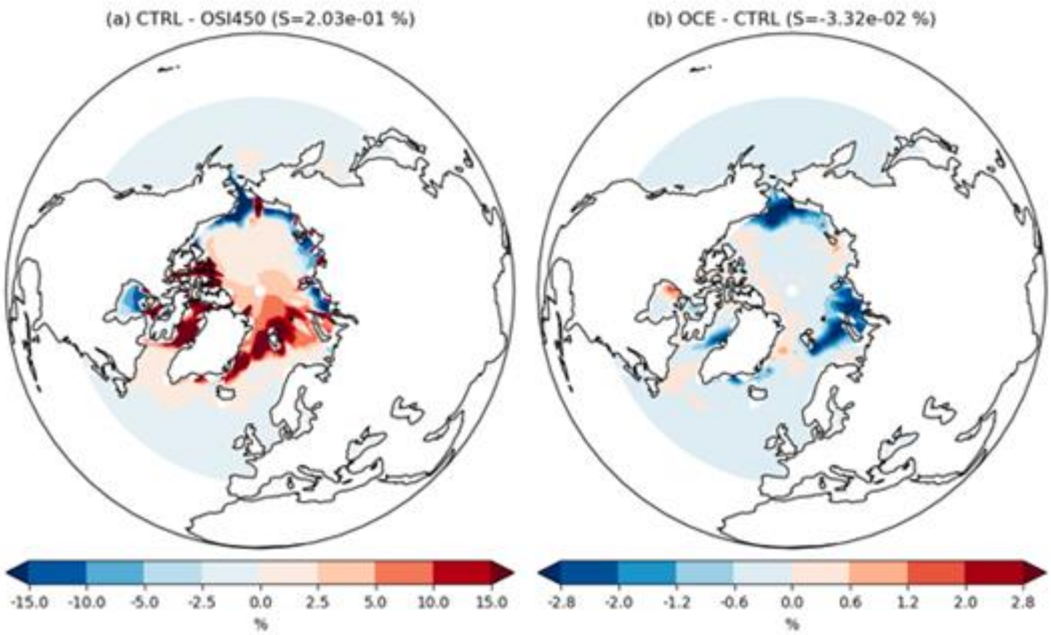

Figure T21.15: *November sea-ice concentration. In (a): the deterministic EC-Earth3P (CTRL) minus the OSI450 observational dataset. In (b): stochastic EC-Earth3P minus deterministic EC-Earth3P. The period is 1980-2015. In (a) is therefore the deterministic model bias, and in (b) how this bias changes when you add stochasticity.*

MPG

There is recent evidence (Li et al., 2019) that models overestimate the impact of deep water formation in the Labrador Sea on the variability of the Atlantic Meridional Overturning Circulation (AMOC). Based on the PRIMAVERA stream1 (WP6) and frontier (WP4) control-1950 simulations, we assess the relative impact of deep water formation in the Labrador and Irminger Sea as well as of the overflow through Denmark Strait and Faroe-Shetland-Channel on AMOC variability across different model resolutions. At the current state, only simulations with our own model (MPI-ESM) applying three different ocean grid configurations (1 degree, 0.4 degree, 0.1 degree resolution) have been used (Figure T21.16), but the study will be extended across all PRIMAVERA models.

For a relative coarse resolution (1 degree), the deep water formation in the Labrador Sea indeed shows the largest impact on AMOC variability. Also deep water formation in the Irminger Sea has a relatively large influence. Regarding the Nordic Seas overflows, only a minor impact of the Denmark Strait overflow and no significant impact of the Faroe-Shetland-Channel overflow on AMOC variability is found for the relative coarse resolution.

With increasing resolution, the dominant impact of the deep water formation in the Labrador Sea vanishes. For the medium resolution (0.4 degree), the influence of Labrador Sea deep water formation and Denmark Strait overflow on AMOC variability is of comparable order. Regarding the Faroe-Shetland-Channel overflow for this resolution, significant correlations are only found when the AMOC is leading, likely indicating the influence of the AMOC on temperature and salinity in the northeastern North Atlantic and thus on the pressure gradient across the Iceland-Scotland-Ridge.

For the highest resolution (0.1 degree), no significant impact of deep water formation in the Labrador Sea on AMOC variability is found. This resolution is also the only resolution where a clear impact of the Faroe-Shetland-Channel overflow on AMOC variability is seen. To the latter result, likely a better representation of the flow path of Iceland Scotland Overflow Water contributes.

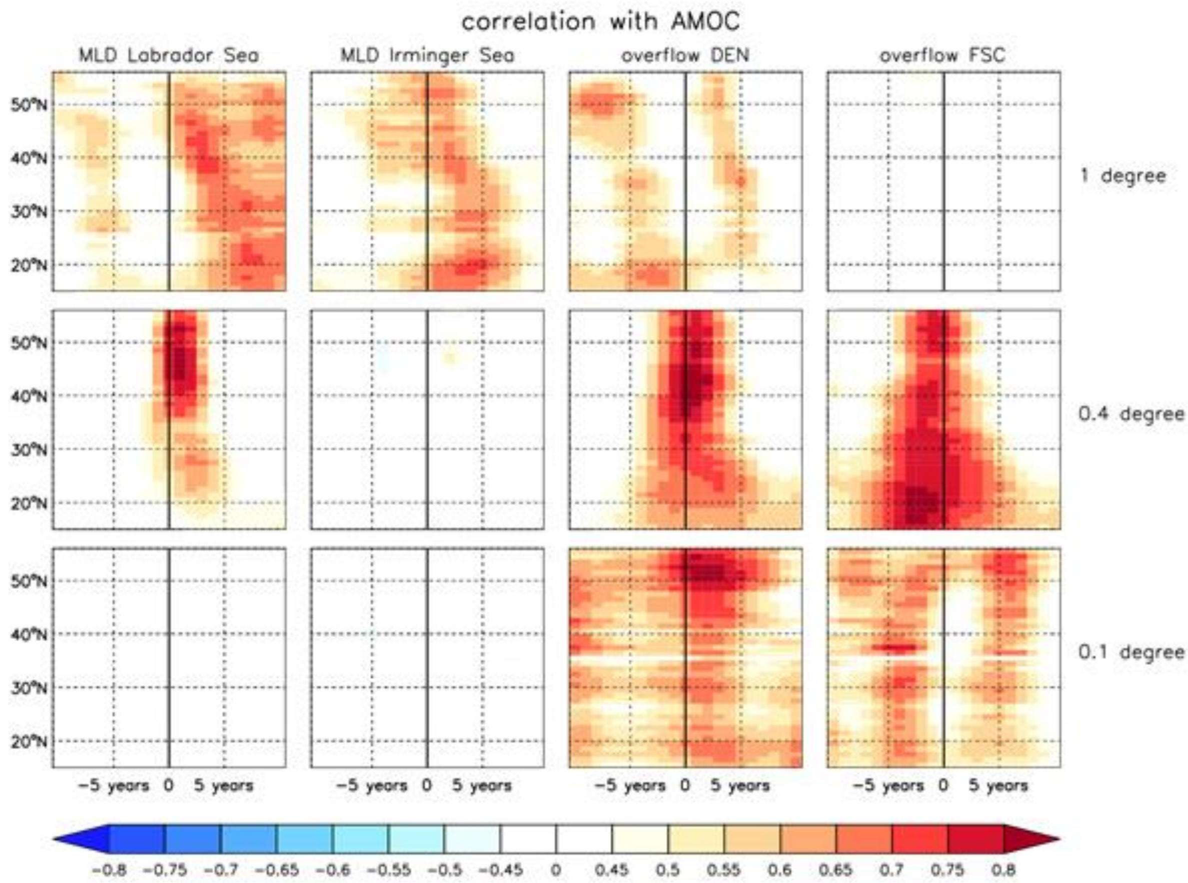

Figure T21.16: *Lag correlation analysis between the maximum AMOC strength at different latitudes and respectively the mixed layer depth in the Labrador Sea, the mixed layer depth in the Irminger Sea, the overflow transport through Denmark Strait and the overflow transport through Faroe-Shetland-Channel for the different ocean grid configurations. Positive (negative) lags indicate that AMOC is lagging (leading).*

CERFACS

Air-sea interactions over GS: Recent observational studies have revealed a band of enhanced convergence over the GS. The mechanisms relating this surface wind divergence/convergence to the SST front remain highly debated. One is the downward momentum or vertical mixing mechanism (VMM), in which the near-surface wind divergence should be proportional to the downwind SST gradient (DWSST hereinafter). A second mechanism is the pressure adjustment (PAM) in which the near-surface wind convergence is shown to be proportional to the SLP Laplacian (LAP(SLP)). Observational and modelling studies show that both mechanisms can play a role depending on the time scale considered, on the resolution of the data that are used, etc. Our objective is to investigate the role of these mechanisms in shaping the surface wind convergence over the GS, aimed at better characterizing air-sea interactions over the GS. We use the PRIMAVERA-AMIP experiments carried out with the LR and HR configurations of the atmospheric component of the CNRM-CM6 coupled model forced by HadISST SSTs over the period 1950-2014. Two ensembles of ten members have been performed with the LR (~140km) and HR (~50 km) versions to accounting for internal climate variability in the analysis. We use as reference dataset the newly developed ERA5 reanalysis and compare ERA5 with respect to HR/LR atmospheric models. Winter mean (DJF) of turbulent heat fluxes reveal that both LR and HR models largely overestimate ERA5 values.

A further analysis of the probability distribution function indicates that this is principally due to stronger extreme values for the models (not shown). Moreover, LR and HR present stronger near convergence values than ERA5, representing 20% larger with respect to the reanalysis. On the other hand, no significant differences are found between both model versions.

To investigate the role of VMM and PAM, we use the conditional mean method, introduced by O'Neill et al. (2017) to study the influence of one variable on the time-mean divergence. Daily divergence fields and winds averaged separately for positive and negative values of the DWSST and LAP(SLP) respectively (figure T21.17). The pattern of wind divergence changes for positive and negative LAP(SLP) indicating a clear influence of PAM on the time-mean convergence (Fig T21.17a). Anomalous wind also influences the divergence field: divergence near the coast is associated with anomalous north-westerly winds. There is also a clear influence of DWSST on time-mean divergence, with almost all the divergence field explained by positive DWSST values and vice-versa (Fig. T21.17b). In the VMM we observe a strong influence of anomalous wind conditions: divergence occurs under anomalous north-westerly winds (strengthening of the mean flow), convergence for anomalous south-westerly winds (weakening of mean flow). Both mechanisms are well represented in HR and LR models, though simulated convergence and divergence are overestimated compared to ERA5. Concerning the role of the model resolution, no significant differences are found in this study and both model configurations display the similar contributions of these two mechanisms to the time-mean divergence.

(a)

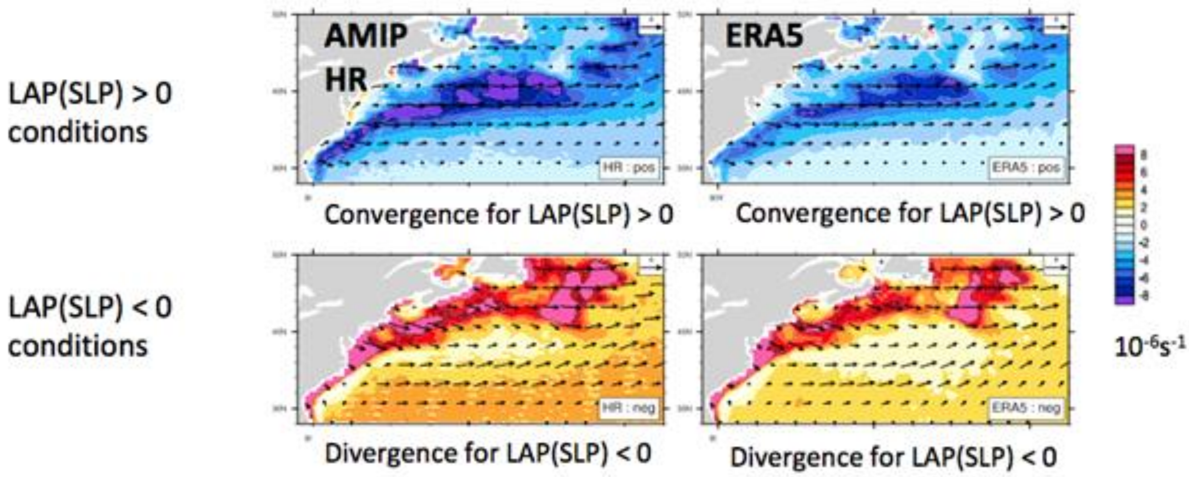

(b)

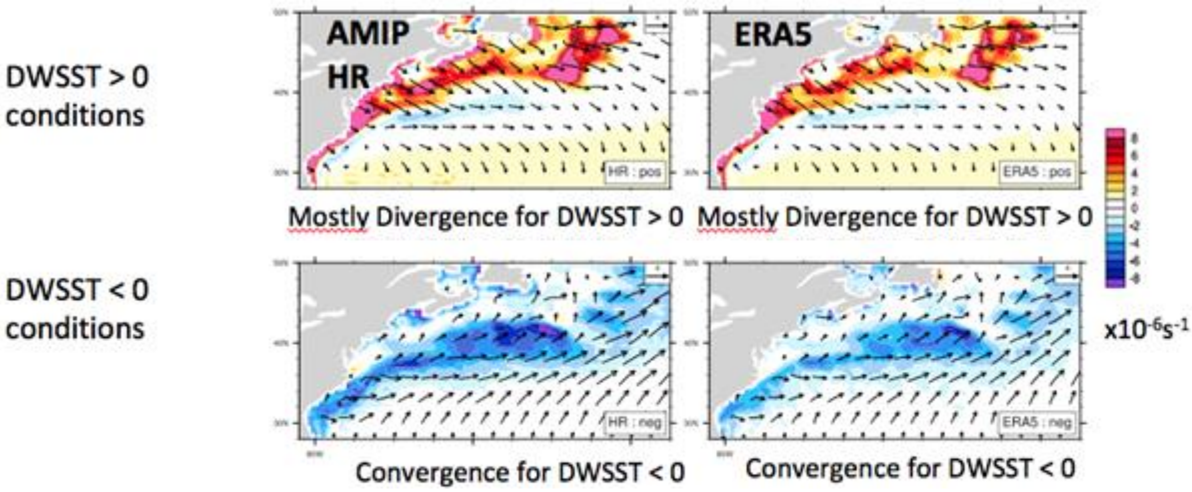

Figure T21.17: *(a) Conditional mean of divergence field (negative for convergence) for positive and negative LAP(SLP) for HR models and ERA5 reanalysis. (b) Conditional mean of divergence field (negative for convergence) for positive and negative DWSST for HR models and ERA5 reanalysis. For HR model the ten members are taken into account.*

Summer Temperature trends in Europe: Past studies have concluded that climate models of previous generations tended to underestimate the large warming trend that has been observed in summer over western Europe. We have studied the role of large scale atmospheric circulation in the North-Atlantic / European sector in that context (Boé et al. 2020). As an ensemble, PRIMAVERA climate models warm less over western Europe and warm more over eastern Europe than observed on the 1951-2014 period, but they generally remain consistent with observations given the large impact of internal variability on trends. These differences in temperature trends are explained to an important extent by an anti-correlation of sea level pressure trends over the North Atlantic / Europe domain between models and observations. The observed trend tends to warm (cool) western (eastern) Europe but the simulated trends generally have the opposite effect. Neither a higher resolution nor the realistic representation of the evolution of sea surface temperature and sea ice leads to a better simulation of sea level pressure trends.

NERC

Boreal winter ocean surface and mid-latitude storm related changes associated with moving from eddy-permitting (1/4º) ocean to eddy-resolving (1/12º) ocean have been examined in control and global warming (RCP8.5) simulations of the HadGEM3 3.1 model in which the atmosphere resolution is kept constant at 25km. The differences in the depiction of the Gulf Stream (Fig. T21.18) were broadly expected from previous eddy-resolving ocean-only model results. Additionally, the revised location of Gulf Stream in ocean resolution affects North Atlantic winter air-sea fluxes and climate, with implications for the future projections of mid-latitude storms (Fig. T21.18).

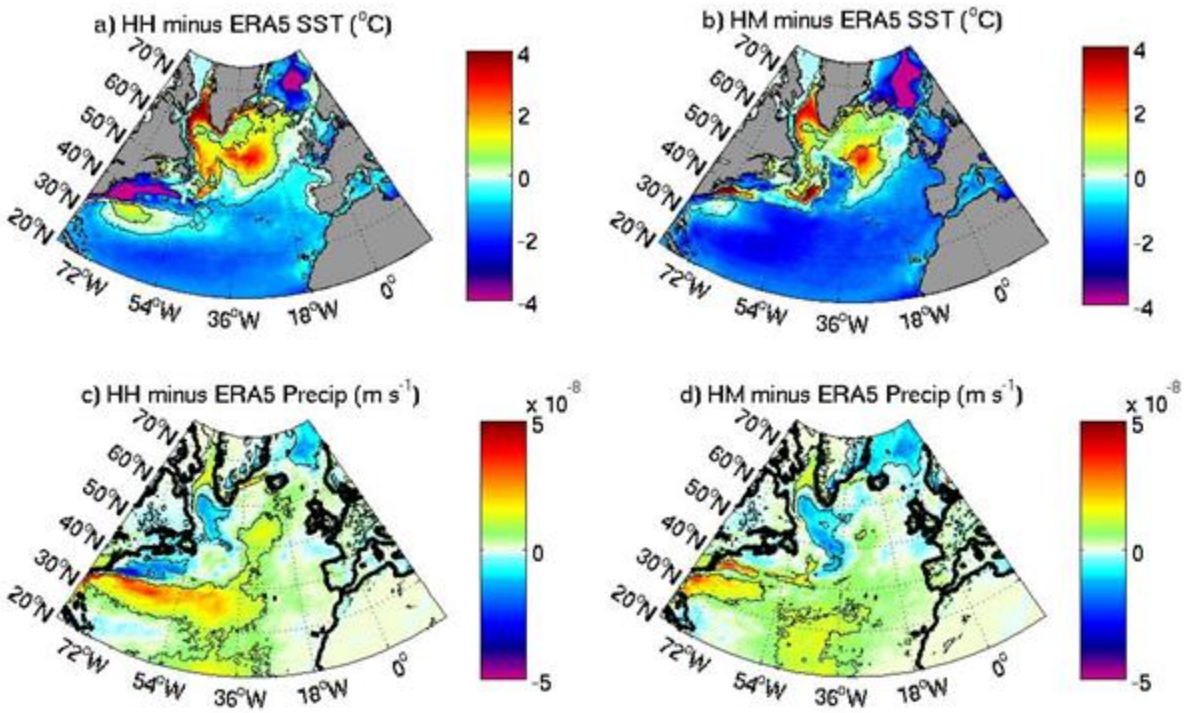

Figure T21.18: *Difference between the HadGEM3 3.1 control runs of eddy-resolving (HH) and eddy-permitting (HM) simulations and ERA5 observations for DJF SST (a) and (b) and precipitation (c) and (d).*

AWI

We investigated the effect of using different combinations of horizontal resolutions in atmosphere (T127 and T63) and ocean (HR and LR) on the simulated climate in AWI-CM. Particular attention was given to the Atlantic Meridional Overturning Circulation (AMOC). Four experiments with different combinations of relatively high and low resolutions in the ocean and atmosphere were conducted. It was shown that increases in atmospheric and oceanic resolution have clear impacts on the simulated AMOC which are largely independent. Increased atmospheric resolution leads to a weaker AMOC. It also improves the simulated Gulf Stream separation; however, this is only the case if the ocean is locally eddy resolving and reacts to the improved atmosphere (Fig.T21.19).

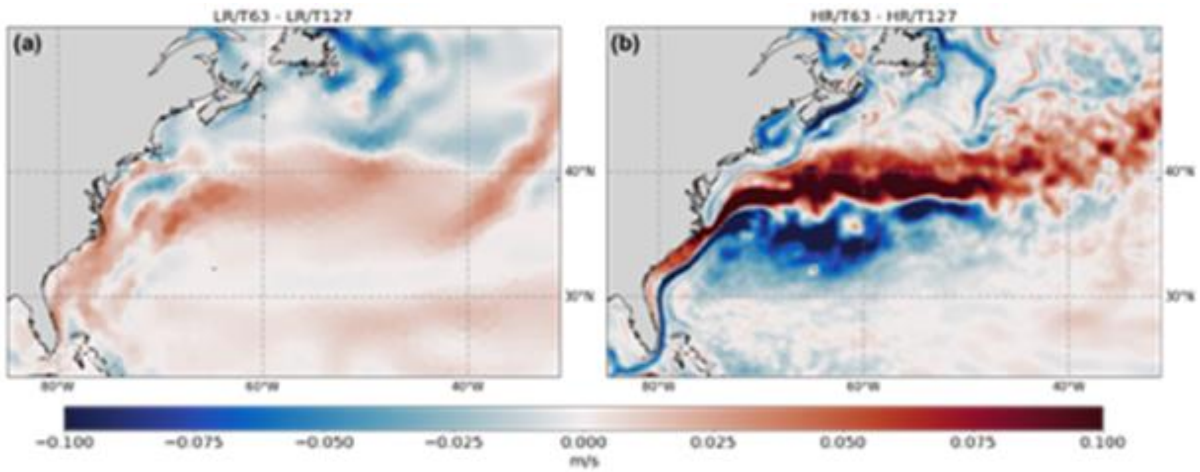

Figure T21.19. *Ocean 50 m velocity differences. Left: LR/T63 – LR/T127, right: HR/T63 – HR/T127.*

We argue that our results can be explained by reduced mean winds caused by higher cyclone activity. Increased resolution of the ocean affects the AMOC in several ways, thereby locally increasing or reducing the AMOC. The finer topography (and reduced dissipation) in the vicinity of the Caribbean basin tends to locally increase the AMOC. However, there is a reduction in the AMOC around 45°N which relates to the reduced mixed layer depth in the Labrador Sea in simulations with refined ocean and changes in the North Atlantic Current pathway.

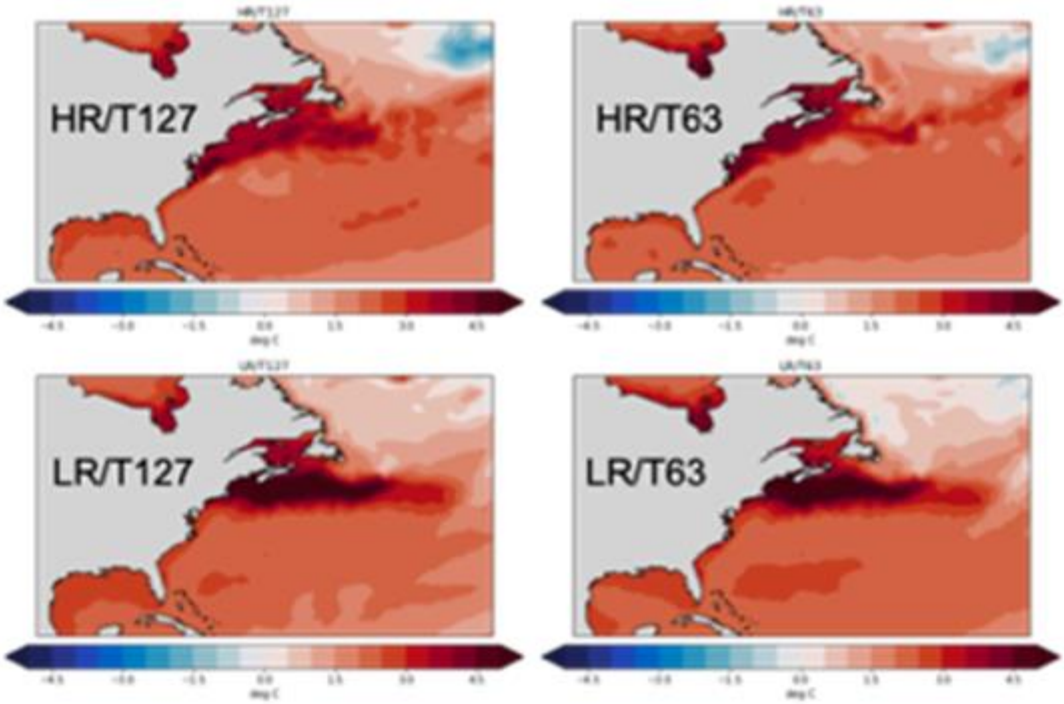

Figure T21.20. *SST change (2070-2099 – 1976-2005)*

Higher ocean resolution also leads to different climate change signal (compared to LR) in the North Atlantic. As illustrated on Fig. T21.20 the differences between LR and HR are mainly located in the North Atlantic Current and Subpolar Gyre regions. It indicates the different Gulf Stream / North Atlantic current response to global warming in HR and LR setups.

3.2 Task T2.2

Summary

Arctic processes play a key part in the global climate through the ocean and the sea ice. The climate warming strongly modifies the Arctic for example via important losses in sea ice or an increase in the poleward ocean heat transport. Including a better representation of these processes is therefore essential for a better understanding of the current and the future climate. The added value of a finer resolution on Arctic sea ice area and volume, the Arctic ocean circulation, the Atlantic Ocean heat transport, the freshwater content, and the Arctic ocean modelling, are summarized below.

The increase of atmospheric or oceanic resolution does not lead to the same results in the Arctic sea ice. Indeed, a finer oceanic resolution contributes to a decrease in Arctic sea-ice area and volume, but the impact of a finer atmospheric resolution is not clear (UCLouvain). This is consistent with less sea ice extent modelled in the high resolution of CNRM-CM6-1 (CERFACS). However, when focusing on a specific sea such as the Barents Sea, the impact of ocean resolution on the March sea-ice area is not as clear-cut (UCLouvain).

Increasing the ocean resolution leads to an increase in the mean poleward Atlantic oceanic heat transport for HadGEM3-GC3.1, ECMWF-IFS and AWI-CM-1-1 (Docquier et al., 2019), in closer agreement with the OHT estimates from Trenberth and Fasullo (2017) (UCLouvain). As for the Arctic sea ice area and volume, the role of atmospheric resolution is less clear. The impact of model ocean resolution is clear when looking at pan-Arctic sea-ice area and Atlantic Ocean heat transport, but this impact is less obvious looking only at the Barents Sea. Therefore, looking at the different Arctic seas separately is important.

The high resolution significantly improves the model's representation of the Arctic Ocean. The most pronounced improvement is in the Arctic intermediate layer, in terms of both Atlantic Water mean state and variability (AWI). Moreover, a better representation of the different ocean currents in the North Atlantic and in the Barents Sea is seen with a finer ocean resolution and requires at least 0.25° to clearly distinguish them (UCLouvain).

As for the Arctic sea ice area and the Atlantic Ocean heat transport, the increase of atmospheric or oceanic resolution does not lead to the same results in the freshwater content (SMHI). A finer atmospheric resolution leads to a higher freshwater volume over the Beaufort Sea and lower freshwater volume over the Laptev and East Siberian. A finer oceanic resolution leads to a lower freshwater volume over the Arctic. Other results show that increasing the atmosphere resolution reduces the ice transport across the Farm strait and the convection at the Labrador Sea (SMHI). Increasing the ocean model resolution reduces the ice export from the Arctic towards the Atlantic (SMHI).

The cold surface air temperature bias over the Arctic is less pronounced in high resolution (oceanic and atmospheric) in CNRM-CM6.1 (CERFACS) which is consistent with less sea ice extent in this resolution. Furthermore, the high resolution exhibits a much more realistic polar vortex variability than low resolution, which can explain why high resolution shows a more rapid and significant response in the stratosphere to the sea ice reduction (CERFACS).

UCLouvain

Arctic sea ice and Atlantic Ocean heat transport.

In HadGEM3-GC3.1, ECMWF-IFS, EC-Earth3P, CNRM-CM6-1 and AWI-CM-1-1, increasing the ocean resolution generally leads to reduced Arctic sea-ice area and volume. In CMCC-CM2, and ECMWF-IFS, the Arctic sea-ice area and volume increase with a higher atmospheric resolution, while these quantities decrease for HadGEM3-GC3.1. For MPI-ESM1.2, the Arctic sea-ice area increases with higher atmospheric resolution and the volume decreases. These results suggest that a finer ocean resolution generally leads to a decrease in Arctic sea-ice area and volume, but the impact of a finer atmospheric resolution is not clear (Docquier et al., 2019; extended with results from EC-Earth3P and CNRM-CM6-1). However, when focusing on the Barents Sea, the impact of ocean resolution on March sea-ice area is not as clear-cut, with a decrease in area for HadGEM3-GC3.1 and ECMWF-IFS, and an increase in area for EC-Earth3P, CNRM-CM6-1 and AWI-CM-1-1 with a finer ocean resolution (Docquier et al., under review).

Increasing the ocean resolution leads to an increase in the mean poleward Atlantic OHT for HadGEM3-GC3.1, ECMWF-IFS and AWI-CM-1-1 (Docquier et al., 2019), in closer agreement with the OHT estimates from Trenberth and Fasullo (2017). The role of atmospheric resolution is less clear. The trends in Atlantic OHT at 50°N, 60°N and 70°N from 1979 to 2014 decrease with an enhanced ocean resolution. The trend is mainly significant at 70°N, where less positive values are observed at finer ocean resolution. This smaller positive trend in OHT at higher ocean resolution can be related to less negative trend in sea ice area and volume at higher ocean resolution. The mean SST and ocean surface velocity in the North Atlantic increase with finer ocean resolution and the complex ocean surface circulation of the Barents Sea requires an ocean resolution of at least 0.25° to clearly distinguish the different ocean currents flowing to the Barents Sea, especially the Atlantic Water and Norwegian Coastal Current (Fig T22.1). For HadGEM3-GC3.1, ECMWF-IFS, AWI-CM-1-1, CNRM-CM6-1 and EC-Earth3P, an increase in OHT at the Barents Sea Opening (BSO, Atlantic Water) is observed at higher ocean resolution, in much better agreement with observations compared to lower resolution (Docquier et al., under review). However, this systematic impact is less clear when looking at the full BSO transect.

In summary, the impact of model ocean resolution is clear when looking at pan-Arctic sea-ice area and Atlantic OHT (Docquier et al., 2019), but this impact is less obvious looking only at the Barents Sea. Therefore, looking at the different Arctic seas separately is important. A clear improvement of an increase of the ocean resolution is the better representation of the different ocean currents in the North Atlantic (Docquier et al., 2019) and in the Barents Sea (Docquier et al, under review).

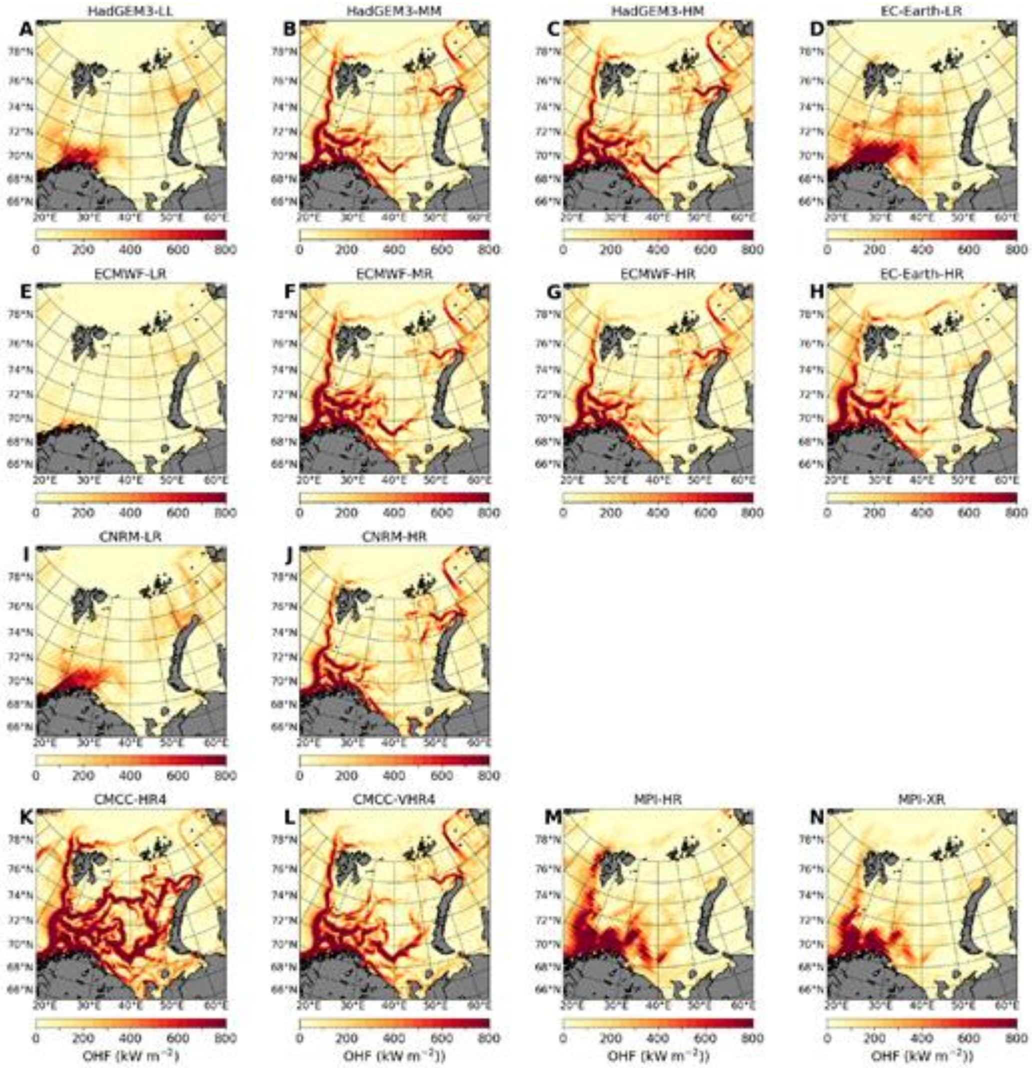

Figure T22.1: *Mean horizontal ocean heat flux (OHF) in the Barents Sea from HighResMIP hist-1950 model outputs, averaged over 1950-2014.*

AWI

Arctic Ocean modelling. To explore the value of using high horizontal resolution for Arctic Ocean modelling, we use two global meshes differing in the horizontal resolution only in the Arctic Ocean (24 km vs. 4.5 km). The high resolution significantly improves the model's representation of the Arctic Ocean. The most pronounced improvement is in the Arctic intermediate layer, in terms of both Atlantic Water (AW) mean state and variability. The deepening and thickening bias of the AW layer, a common issue found in coarse-resolution simulations, is significantly alleviated by using higher resolution. The topographic steering of the AW is stronger and the seasonal and interannual temperature variability along the ocean bottom topography is enhanced in the high-resolution simulation. The high resolution also improves the ocean surface circulation, mainly through a better representation of the narrow straits in the Canadian Arctic Archipelago (CAA). The representation of CAA through-flow not only influences the release of water masses through the other gateways but also the circulation pathways inside the Arctic Ocean. However, the mean state and variability of Arctic freshwater content and the variability of freshwater transport through the Arctic gateways appear not to be very sensitive to the increase in resolution employed here.

SMHI

Freshwater content in Arctic

In order to better understand the changes in freshwater content (FWC) produced by changes in the model resolution, we calculated the difference in FWC between low and high resolutions for each model (Fig.T22.2). High-resolution simulations were interpolated to the low resolution using cubic interpolation. When low and high ocean resolution simulations (ORCA1 minus ORCA025) are compared, we find that low resolution shows larger FWC over the Central Arctic Ocean and lower FWC over the Kara and Laptev Seas compared with high resolution. In turn, when lower and higher atmosphere resolutions in the HadGEM simulations are compared, we find that lower resolution shows increased FWC over the Kara and Laptev Seas and decreased FWC over the Beaufort Sea. This result is systematic since the lowest and highest resolution shows the largest FWC difference.

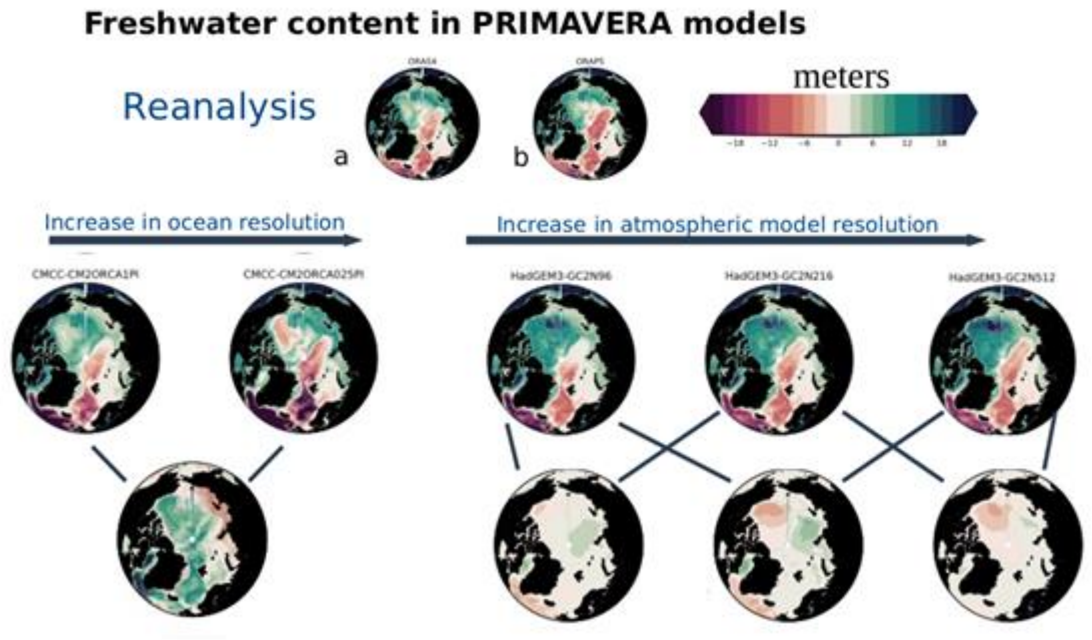

Figure T22.2: *Freshwater content in PRIMAVERA models*

In general GCMs have a dependency on model resolution, showing with an increased atmospheric model resolution a) Higher freshwater volume over the Beaufort Sea and lower freshwater volume over the Laptev and East Siberian Seas, b) Lower ice transport and higher freshwater transport across the Farm strait, c) lower convection at the Labrador Sea. Increased ocean model resolution models show: a) Lower freshwater and ice volumes over the Arctic, b) Lower ice export from the Arctic towards the Atlantic, c) Higher freshwater transport across Fram strait and lower freshwater export across the Baffin Bay. All the previous results also showed some model dependency

CERFACS

Atmospheric mean state and variability affecting the response to the Arctic sea ice decline

The atmospheric response to the Arctic sea ice decline has been analysed and compared in the LR and HR versions of the coupled model CNRM-CM6.1. On this purpose we use the idealised sea ice albedo experiments designed and performed in PRIMAVERA/WP5.

The results of LR/HR atmospheric response to the idealised Arctic sea ice decline will be presented and discussed in more detail in the incoming deliverable D5.3. In these experiments, the albedo of sea ice is reduced to the ocean value, and an ensemble of 200 members initialised from the control-1950 experiment and considering this albedo perturbation has been conducted. Please note that initially the PRIMAVERA protocol agreed on 40 members. But further analysis has revealed that more members are needed to obtain a robust and significant response either at the surface or in upper levels, in particular at the stratosphere. In general, both LR and HR show very similar responses at the surface (sea level pressure and 2m temperature) and in upper atmospheric levels. However, for the case of HR, fewer members are necessary to exhibit a significant atmospheric response at the surface and also a signal in the stratosphere. Here we have analysed the mean state and variability simulated by both model versions and compared them to ERAI reanalysis. Indeed, we argue that the mean climate background and variability as simulated by each model can affect the atmospheric response and its statistical significance to the Arctic sea ice loss. We have evaluated LR and HR models in terms of the mean and standard deviation of sea ice extent (SIE), 2m temperature (SAT), and zonal winds at 200 hPa (U200) and 10 hPa (U10). These variables are important to understand the atmospheric response (troposphere and stratosphere) to Arctic sea ice decline. In general, HR exhibits lesser SIE compared to LR for the whole Arctic. Both models show a cold SAT bias over the Arctic region, but LR biases are larger with respect to ERAI. The cold bias reduction in HR is coherent with less SIE in this model. Regarding the dynamics, LR and HR models show a more pronounced and variable jet stream (zonal wind at 200 hPa) compared to ERAI. In particular, HR biases are enhanced (Figure T22.3). In the stratosphere, the polar vortex strength is also overestimated in both models, but HR exhibits a much more realistic polar vortex variability than LR. In summary, mean state and variability of HR and LR affect the atmospheric teleconnection mechanisms associated in the atmospheric response to the Arctic sea ice decline. HR and LR biases in mean and standard deviations are different in temperature and dynamical variables and also depend on the atmospheric level considered. In general, HR shows a more realistic polar vortex than can explain why HR shows a more rapid and significant response in the stratosphere to the sea ice reduction. These results will be included in an incoming paper (Chripko et al., in prep).

(a)

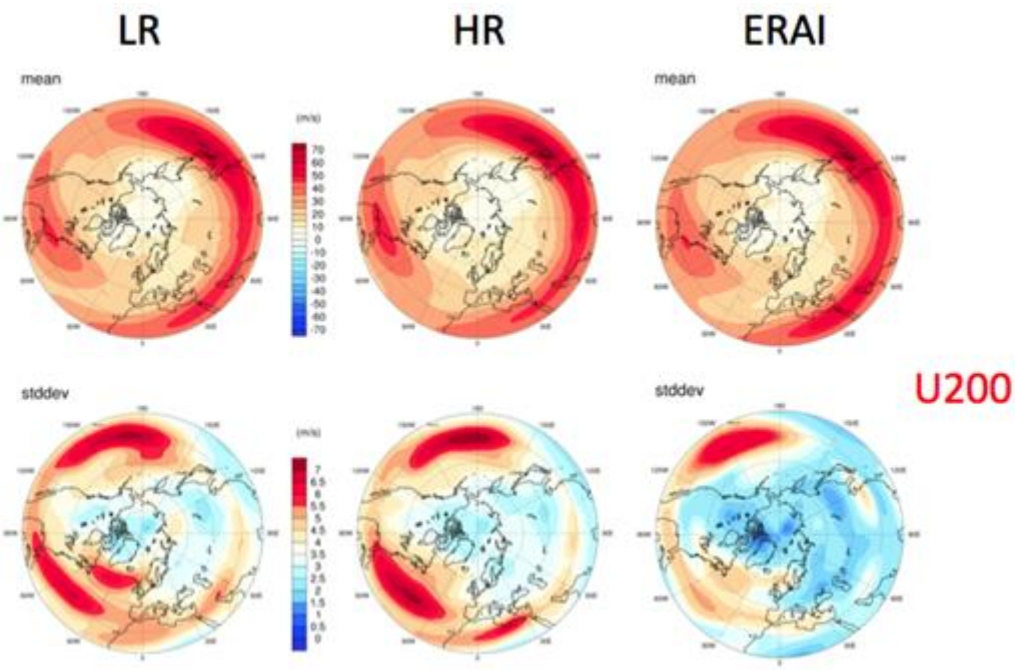

(b)

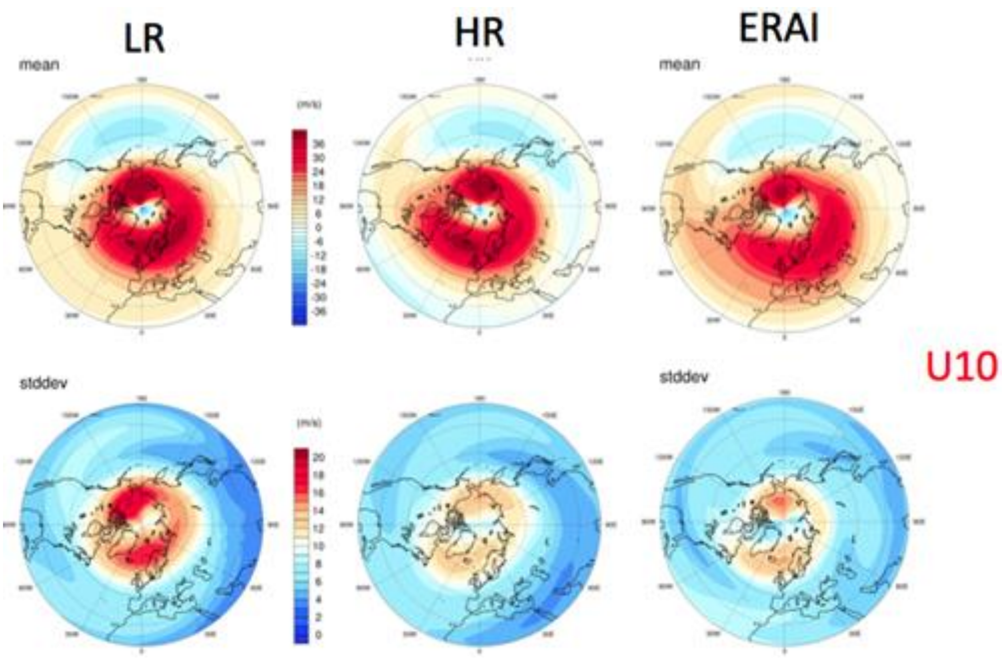

Figure T22.3: *winter mean and standard deviations for LR and HR versions of the coupled model CNRM-CM6.1 and ERAI reanalysis for (a) jet stream (zonal wind at 200 hPa) and (b) stratospheric polar vortex (zonal wind at 10 hPa). The diagnostics are computed from the control-1950 experiment.*

3.3 Task 2.3

Summary

There has been a number of studies looking into the impact of horizontal resolution on simulated tropical cyclone (TC) activities in recent years (e.g. Caron et al. 2011; Strachan et al. 2012; Wehner et al. 2014; Roberts et al., 2015; Vecchi et al. 2019). Although they vary in their approach, these studies have generally shown an improvement in the number and the geographical distribution of tropical cyclones with resolution. Roberts et al. (2020a) showed that these improvements were also present in PRIMAVERA GCMs. The increase in resolution generally leads to an increase in activity in all major basins supporting TC formation, with the largest increase detected over the western North Pacific and the eastern North Pacific. This increase in activity is driven by an increase in the number of cyclogenesis events and leads to a general improvement in simulated TC activity (Met Office). The improvement over the eastern Pacific is not entirely unexpected due to the fact that, on average, storms forming over that area tend to be smaller than in other basins and because a significant fraction of TC development in that basin occurs through interaction of Atlantic tropical waves with Central American orography (Zehnder et al., 1999), which is better represented at higher resolution.

However, while we detect an improvement in the mean track density of the multi-model ensemble, individual models show widely different responses to increased resolution: two models show a strong increase in activity (HadGEM3-GC31, CMCC-CM2), while two others display only a very small sensitivity to resolution (ECMWF-IFS; MPI-ESM) and one (CNRM-CM6-1) even shows a decrease in activity over certain basins (Met Office). It's worth highlighting that the two GCMs (HadGEM3-GC31 and CMCC-CM2) that show the strongest response to resolution are grid-point models while all the other models are spectral models, strongly suggesting that the sensitivity to resolution is dependent on the model formulation.

While the northern Atlantic is the basin showing the smallest increase and arguably smallest improvement with resolution (particularly in coupled mode), there is a very clear improvement in the representation of storms undergoing extra-tropical transition (U. Reading) and, for at least one model, in the latitudinal distribution of the residence time (CMCC) over that basin. By examining the structural evolution of tropical cyclones, Baker et al. (2020) showed that the negative ensemble-mean bias in track density for storms acquiring frontal, cold-core structures (vs the mean track density field of seven reanalyses) in low-resolution models is significantly reduced at high resolution in both atmosphere-only and coupled simulations . This improvement is driven by a reduction in the cyclogenesis density bias, which is also reduced at higher resolution (U. Reading).

Over the same basin, the representation of meridional transport of water shows a limited improvement with the increase in resolution, at least in the CMCC-CM2 model where this was evaluated. Generally, the CMCC-CM2 model shows an integrated meridional water vapor (IMVT) transport peak further south than observed and only the high-resolution atmosphere-only configuration of the CMCC-CM2 model reaches a reasonably good representation of observed IMVT latitudinal distribution (CMCC).

We also generally note an increase in TC-related precipitation with resolution in all models (Vannière et al., 2020). This increase is mostly driven by the change in frequency of tropical cyclones when resolution is increased. For some models, this increase is slightly offset by a decrease in the amount of precipitation per TC at higher resolution, a reduction which is the result of fewer TCs with low precipitation in LR compared to HR, which lead to higher precipitation per TC on average at LR. The Western Pacific is one of the regions with the largest increase in TC activity. The CMCC-CM2 model in particular is one of the models showing a strong increase in typhoon activity and typhoon-related precipitation over that region. This improvement in the representation of typhoon activity allowed Scoccimarro et al. (2020) to capture the typhoon-induced drying of the Maritime Continent that occurs during the most active typhoon seasons (CMCC). This signal, which is caused by a net reduction in westward water flow into the Maritime Continent atmosphere during those active years, is completely absent in the lower resolution version of their model.

By comparing the precipitation and the moisture budget of tropical cyclones within a 5º radial cap of the storm centre (noted TCP5º) in LR and HR, Vannière et al. (2020) showed that precipitation can be relatively insensitive to the grid horizontal resolution for the more intense system. While precipitation intensity increases near the centre of the storm (<1deg) with resolution, for some models, this is compensated by a decrease in intensity further away from the centre (>1deg, <5deg), leading to a redistribution of the precipitation within the TCs. Vannière et al. (2020) showed that this relatively low sensitivity to resolution is because the TC precipitation is in balance with the large-scale environment and primarily driven by the intensity of low-level radial wind at the edge of the tropical cyclone, and thus moisture convergence, and independent of the inner core dynamics. On the other hand, TCP5º for the weaker systems is not only sensitive to resolution but also to the choice of the tracking algorithm. However, the fact that these differences decrease when we relax the criterion used to identify TCs strongly suggest that other convective systems compensate for the lack of precipitation in LR and that the difference between LR and HR for low TCP5º can be attributed to tropical vortices not passing the necessary thresholds during the TC identification process (U Reading).

Many previous studies have shown resolution to have a strong impact on the intensity of simulated tropical cyclones (e.g. Caron et al. 2011; Strachan et al. 2012; Roberts et al., 2015). Here, we also note that increasing model resolution improves the relationship between the minimum surface pressure at the centre of the storm and the maximum surface wind speed in the vicinity of the centre. Consequently, we detect an improvement in the capability to represent the spectrum of tropical cyclone intensities: the intensity of the TCs, as measured by the maximum wind speed near the surface, increases from category 1 on the Saffir-Simpson scale, to category 2, 3 or 5, depending on the CGCM and the PDF of the maximum intensity becomes more realistic (Met Office).

Integrated kinetic energy (IKE) is an alternative metric used to assess storm intensity (BSC). This metric, unlike other integrated measures such as accumulated cyclone energy, takes into account the size of the storm and shows a better correlation to TC-related damage than other intensity metrics. More specifically, IKE integrates the kinetic energy of the horizontal wind field of a storm over the area for which the wind field exceeds a certain wind speed threshold (17 m/s in this case). Analysis of the TCs in the CNRM model showed that both LR and HR configurations manage to produce storms of comparable IKE (BSC). However, as one would expect, there is a clear difference between how LR and HR reach similar IKE values: cyclones in HR are generally stronger and smaller than in LR. When computing the total IKE produced over an entire season, large differences between LR and HR emerge however, with HR producing much larger values (not shown). In this case, the differences are driven, not by the differences in the IKE of individual cyclones, but by the differences in the number of cyclones in the two configurations, a result which is reminiscent of TC-induced precipitation discussed earlier (BSC).

Finally, with regard to the impact of increasing GHGs, Roberts et al. (2020b) note an increase over the Atlantic and a decrease over the North Pacific in the atmosphere-only simulations, and a more mixed response in the coupled simulations. If the signal over the Northern Hemisphere is ambiguous, the Southern Hemisphere presents a robust decrease in activity, particularly over the South West Indian Ocean, where TC activity is projected to decline in both LR and HR. This projected decrease in activity has been noted in previous studies as well (Gleixner et al. 2014; Knutson et al. 2019). In the higher resolution simulations, they also note a poleward shift in activity over the western North Pacific, which is consistent with Altman et al., (2018), Kossin et al., (2014, 2016) and Sharmila & Walsh, (2018). However, they found little to no change in 10m wind speeds between future and present climates, although a small increase in 10m wind speeds is found in the coupled models presenting smaller present-day biases (Met Office).

The models so far analysed following the CMIP6 HighResMIP protocol show a wide variety of behaviours, with some models in the 20-50 km resolution range able to represent observed tropical cyclone frequency, spatial distribution and even intensities. The North Atlantic remains particularly challenging, even at higher resolution, where the TC frequency is consistently biased low, although we see significant improvement in the representation of extra-tropical transitions and TCs' residence time latitudinal distribution for that region. These results are generally robust across tracking algorithms, although the differences between resolutions are larger in TempestExtremes (Ullrich and Zarzycki, 2017) compared to TRACK (Hodges et al. 2017). Some characteristics of tropical cyclones are clearly sensitive to resolution (number of storms, maximum surface wind speed), while others are less so (total precipitation of intense cyclones; IKE) and the strongest differences in TC-related characteristics are typically related to the increase in the number of cyclones with resolution.

CMCC

The low-resolution configuration of the CMCC-CM2 model, namely CMCC-CM2-HR4, underestimates both the number of tropical cyclones (TCs) and the ACE linked to their activity in the West North Pacific area (Figure T23.1, and Scoccimarro et al., 2020). On the contrary, the high-resolution model configuration, namely CMCC-CM2-VHR4, which increases the atmospheric resolution from one degree to one-fourth of a degree, displays values of TCs count and ACE closer to observation, even if biases remain (Figure T23.1). Given the better representation of TCs in the West North Pacific area obtained by the CMCC-CM2-VHR4 model, this high-resolution configuration can reproduce the observed influence of tropical cyclones on the maritime continent drying (Figure T23.2, Scoccimarro et al., 2020). Besides, at high resolution, a more realistic representation of strong tropical cyclones is achieved when a high-frequency coupling between ocean and atmosphere is used (Scoccimarro et al., 2017): with low-frequency coupling, a high resolution (1/4 degree) model tends to overestimate TC intensities due to the missed SST negative feedback.

The increase in atmospheric resolution exhibits an impact on the ability of Global Circulation Models in representing tropical cyclones Residence Time over the North Atlantic basin (Figure T23.3a). The observed tropical cyclones tracks (IBTRAC) show a maximum of residence time in the latitudinal band between 15°N and 35°N (Figure T23.3a). A similar distribution is captured by GCMs, with closer values to observation when high-resolution models are evaluated compared to low-resolution configuration. This feature is consistent in both coupled (hist-1950) and atmosphere-only (highresSST-present) configurations. Besides, the use of observed surface boundary conditions (highresSST-present configuration) leads to further improvement in the simulated Residence Time latitudinal distribution (Figure T23.3a, Peano et al., in prep.).

Tropical Cyclones transport energy and water along their pathways. The water transport associated with TCs is analyzed over the North Atlantic basin by evaluating the latitudinal distribution of integrated meridional water vapor transport (IMVT) associated with TCs. The observed IMVT is computed using IBTRACS for TCs pathways and JRA-55 for meridional velocity and specific humidity fields. Observations exhibit a maximum of IMVT associated with TCs in the latitudinal band between 45°N and 55°N (Figure T23.3b). The CMCC-CM2 model (Cherchi et al., 2019) exhibits maximum values that are too much to the south compared to observation, in the latitudinal band between 35°N and 45°N, but the atmosphere-only high-resolution configuration shows a latitudinal distribution closer to the observed one (Figure T23.3b, Peano et al., in prep.).

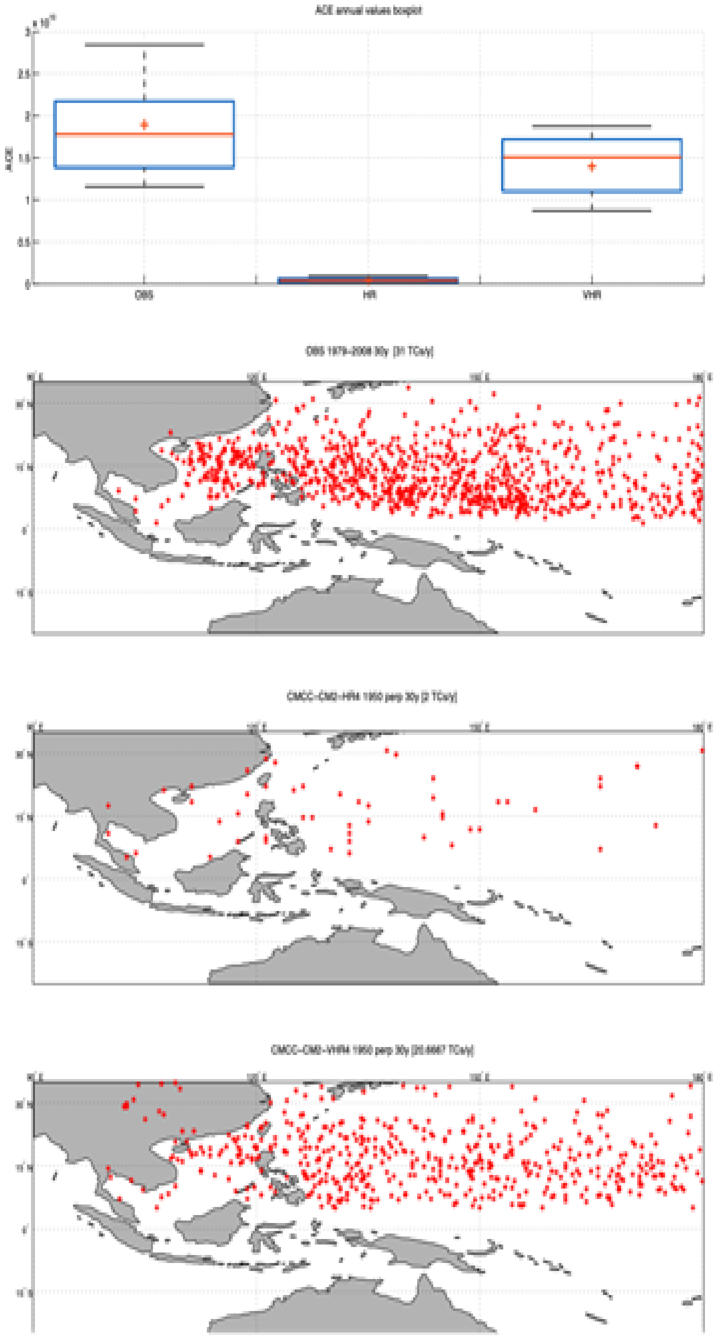

Figure T23.1: Tropical cyclone representation in CMCC-CM2 model. *Upper panel shows the box plot of annual Accumulated Cyclone Energy over the West North Pacific basin, considering 30 years, for observations, CMCC-CM2-HR, CMCC-CM2-VHR in left, central and right boxes respectively. Units are [m2/s]. Panels B, C and D show the geographical distribution of observed and modelled TC genesis location in the 30-year period.*

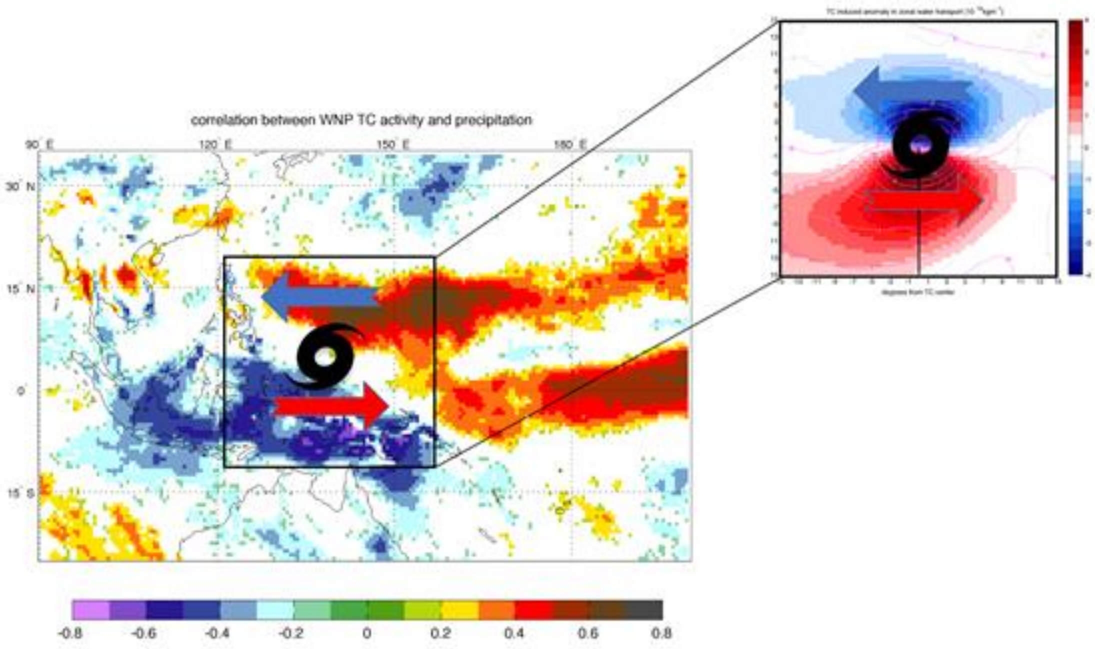

Figure T23.2: Scheme of influence of Tropical cyclones on the maritime continent drying*. Correlation between ACE and precipitation for the 1979-2015 period with average JJA values and TC induced anomaly in zonal water transport.*

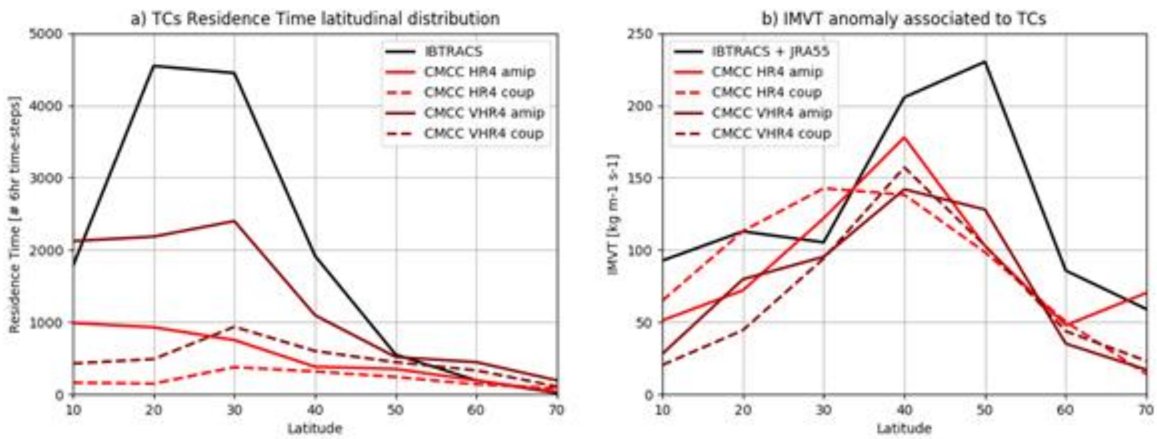

Figure T23.3: Tropical Cyclones Residence Time and Integrated Meridional water Vapor Transport representation in CMCC-CM2 model*. Left panel shows the latitudinal distribution of Tropical Cyclones (TCs) Residence time measured in "number of 6hr time-steps" with tropical cyclones in each latitudinal band of 10 degrees in the period 1985-2014 over the North Atlantic basin. Right panel shows the latitudinal distribution of Integrated Meridional water Vapor Transport (IMVT) associated with TCs (500km radial average along TCs tracks) in the period 1985-2014 over the North Atlantic basin.*

BSC

Commonly used indices to estimate the damage potential of tropical cyclones are the Accumulated Cyclone Energy (ACE) index and the Power Dissipation Index (PDI) which are integrated measures of number, intensity and duration of cyclones. They are typically used to represent the level of activity of a hurricane season. However, ACE and PDI neglect a key factor relating to damages: the actual storm size. Studies by Mahendran (1998), Kantha (2006) and Zhai and Jiang (2014) show that including the storm size and structure is beneficial to damage estimates and the explained variance in associated losses.

To address this issue, a measure called Integrated Kinetic Energy (IKE, Powell and Reinhold 2007), was developed. This metric, unlike other integrated measures such as ACE and PDI, includes the size of the storm by integrating the energy of the entire wind field. IKE is the volume integral of the kinetic energy per volume unit (KE) of the horizontal wind field of a storm and is calculated as the area over which the wind field exceeds a certain wind speed threshold, vertically integrated over a 1-metre layer centred around 10 metres height for which the conditions are considered representative for the entire 1-metre layer:

$$IKE = \int_{[V]} KE \, dV = \int_{[V]} 0.5 * \rho * \sqrt{(u^2 + v^2)}^{\,2} * dV$$

In this study, only grid points with wind speeds larger than 18 ms^{-1}, which is the threshold required for a storm to be classified as a tropical cyclone, contribute to the IKE. Figure T23.4 shows an example of a surface wind speed field associated with a tropical storm. The green dot represents the centre of the storm as identified by the tracker. The yellow isolines display the 18 ms^{-1} isotachs. All the grid points within the isotachs are considered for the IKE computation. The model used to assess the effect of horizontal resolution and climate change on tropical cyclone IKE is the CNRM model, specifically the CNRM-CM6-1 model, but work is underway to extend this study to coupled simulations and other PRIMAVERA GCMs as well.

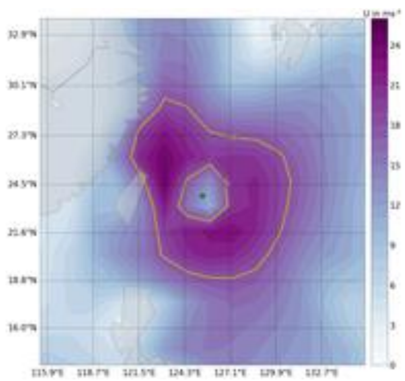

Figure T23.4: *Example of a wind speed field selected by the tracker. The storm centre as detected by the tracker is represented by the green dot. The 18 ms^{-1} isotachs are highlighted in yellow. All the grid points located within the isotachs are taken into consideration when calculating IKE.*

Figure T23.5 shows that there is a higher number of storms in the HR simulation (triangles) and that these are more intense storms (as measured by the maximum surface wind speed) than the storms in the LR simulations (circles): the maximum wind speed associated with maximum lifetime IKE almost doubles from roughly 38 ms^{-1} to about 76 ms^{-1}. It also shows that the largest storms are similar between both experiments, with about 2.6 * 106 km^2 for LR and approximately 2.4 * 106 km^2 for HR. Surprisingly, both configurations also manage to produce storms of comparable maximum IKE. However, a clear difference between LR and HR is the distribution of the data points with storms in HR being shifted toward higher wind speeds and smaller size whereas LR tends to produce larger but weaker storms. The linear regressions (solid and dashed black lines) confirm this difference and reveal that TCs in HR are characterised by a smaller IKE area relative to TCs in LR (at constant wind speed). The blue and red lines, depicting the regressions for storms in the WNP and NA, show a similar behaviour.

To determine whether storm intensity or size is the controlling factor on maximum IKE, the correlations are computed and displayed in Table T23.1. Additionally, the correlation between IKE and the minimum mean sea level pressure (MSLP) of the storm associated with the lifetime maximum IKE is shown. As expected, the correlations show that there is a strong relationship between the quantities and show that storm size is the dominant factor in driving IKE, at both resolutions. Correlations are lower for the wind speed and minimum MSLP, but both still provide an excellent predictor for maximum IKE. Interestingly, MSLP seems to be more correlated to IKE than maximum wind speed at HR, but this is not the case in LR. Although the differences are small, they are consistent across basins. The reason for this is not clear at this stage.

	LR	**HR**
maximum surface wind speed	0.87	0.82
IKE area	0.99	0.96
minimum MSLP	-0.78	-0.85

Table T23.1: *Correlations of maximum lifetime IKE (for the period from 1950-2050) with associated maximum wind speed, IKE area and minimum MSLP for the northern hemisphere.*

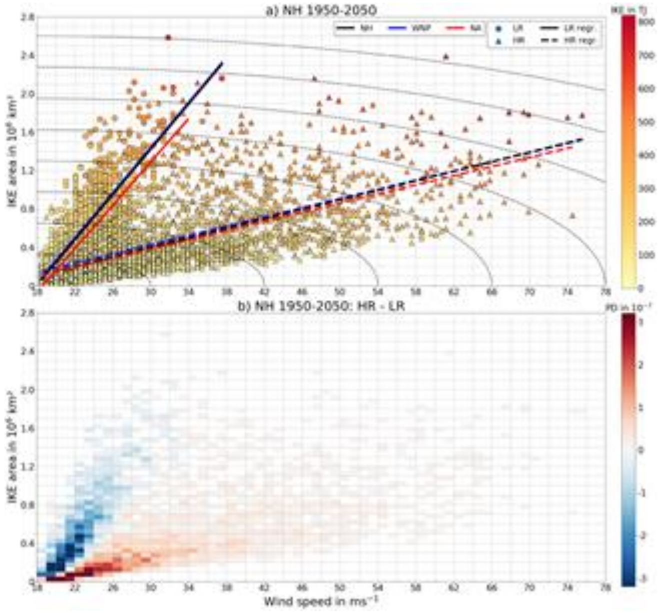

Figure T23.5: *(a) Scatter plot of storm area above 18 ms^{-1} wind speed threshold ("IKE area") against wind speed associated with maximum lifetime IKE of all the storms in the entire northern hemisphere from 1950-2050. IKE values are colour-coded for both resolutions, LR (circles) and HR (triangles). Regression lines (relative to wind speed threshold) are drawn in solid for LR and in dashed for HR. The regressions for the storms attributed to the WNP and NA are shown in blue and red, respectively. The dashed ellipses show an approximation of constant IKE values across the scatter plot. (b) Difference (HR - LR) in joint PD for IKE area and wind speed associated with maximum lifetime IKE of all the storms in the entire northern hemisphere from 1950-2014. The bins are 1 ms^{-1} for the the wind speed and 0.05 * 10^{6} km² for the IKE area.*

MET OFFICE

We have assessed the historic performance of the multi-model PRIMAVERA ensemble of atmosphere-only simulations in Roberts et al. (2020a), using two different tracking algorithms TRACK and TempestExtremes (Fig. T23.6). Most models have higher tropical cyclone frequency with higher resolution, usually an improvement compared to observations. The resolution difference is greatly enhanced using TempestExtremes. The spatial TC patterns also improve across the models, as do the TC intensities, particularly for CNRM-CM6-1-HR which almost matches the observed 10m wind speed-mean sea level pressure relationship. Using HadGEM3-GC31 with a larger number of ensemble members, we demonstrate that the higher resolution models have an improved interannual variability compared to observations.

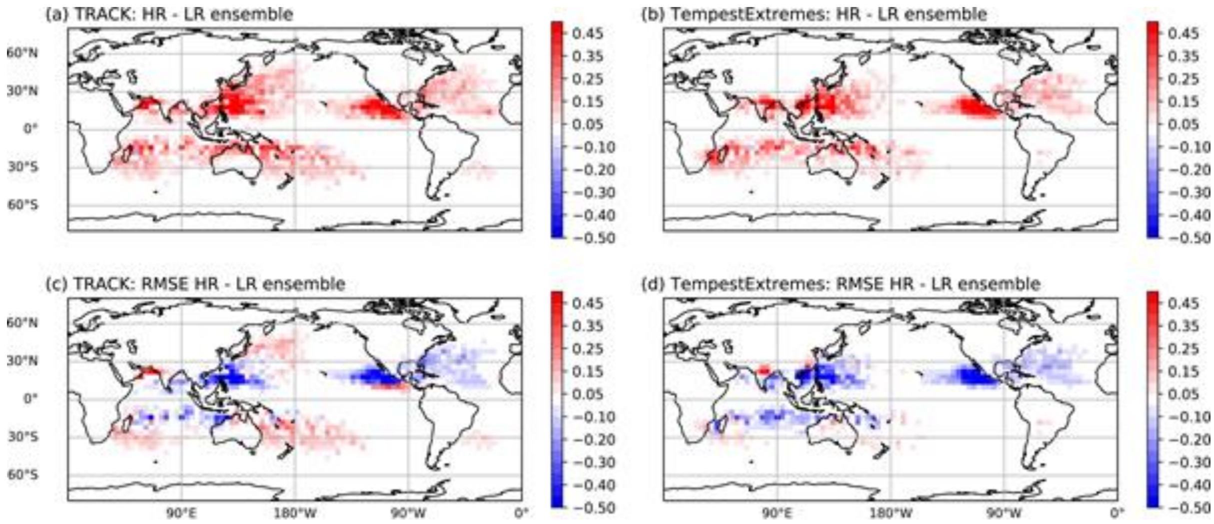

Figure T23.6: *Ensemble mean of the track density (a), (b) difference and (c), (d) RMSE difference between pairs of high- and low-resolution models using (left) TRACK and (right) TempestExtremes.*

The coupled model and projected future change in tropical cyclones have been investigated in Roberts et al. (2020b). The TC frequency also increases with resolution in the coupled models, though for models other than CNRM-CM6-1 there is a low bias in the North Atlantic (Fig. T23.7). Changes in future TC activity in the Northern Hemisphere depend on forcing, with the Atlantic having an increase in the atmosphere-only simulations and the North Pacific a decrease, while the changes are more mixed in the coupled simulations. The Southern Hemisphere has a more robust decrease in activity, particularly in the South West Indian Ocean. There is considerable model agreement about the changes, and the two tracking algorithms give much the same results. Looking at future changes in 10m wind speed shows more resolution dependence in atmosphere-only models, where models with smaller bias have smaller changes in wind speed; changes in coupled 10m wind speed are generally small. Overall these projected future changes are less systematic in the models than in the literature where there is “consensus” that future TCs will have stronger 10m wind on average. Note that this work also included some additional models from outside the PRIMAVERA groups (MRI-CGCM3.2, NICAM16, CESM1.3) from collaborators who had given their TC tracks for the analysis.

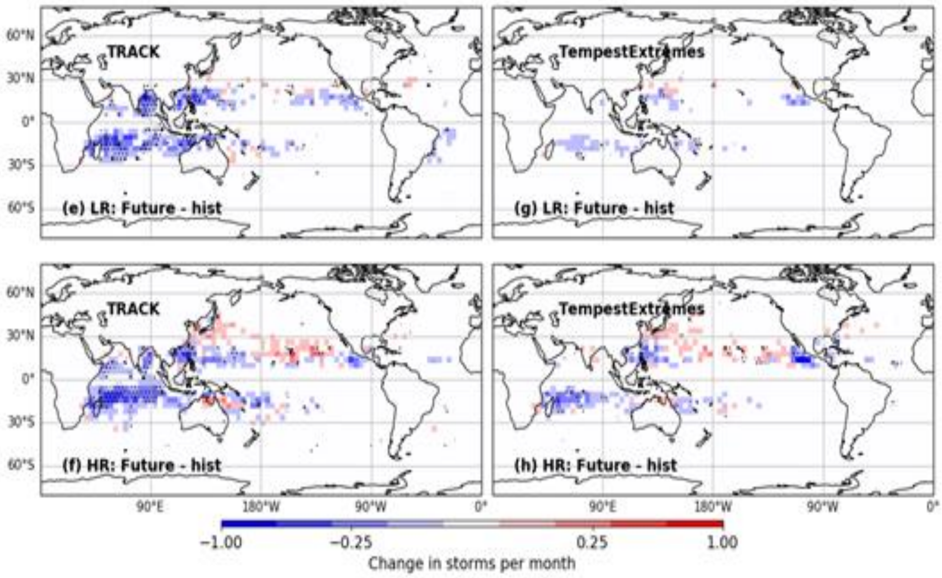

Figure T23.7: *Multi-model mean change in track density between 1950-1980 and 2020-2050, for coupled model experiments, for (left) TRACK and (right) TempestExtremes trackers. Each plot has the mean of the LR models in the upper panel, and the HR models in the lower panel. Small dots indicate where at least 60% of the models agree on the sign of change, and larger dots show where more than 80% of the models agree on the sign of change.*

U READING

Precipitation and moisture budget of tropical cyclones.

We have investigated the sensitivity of precipitation per TC and the TC moisture budget to the horizontal resolution in 5 GCMs of the PRIMAVERA ensemble (CMCC-CM2, CNRM-CM6-1, EC-Earth3P, ECMWF-IF, MPI-ESM1-2) (Fig. T23.8). Using TC tracks obtained with two different tracking algorithms, TRACK and TempestExtremes, allowed us to assess the dependence of the results to the choice of the tracking. Precipitation per TC was diagnosed by averaging precipitation in a 5º radial cap and noted TCP5º. The main results are as follows:

(1) The distribution of TCP5º showed that large TCP5º has little sensitivity to resolution whereas low TCP5º is less frequent in LR models.

(2) Low TCP5º is not only sensitive to resolution but also to the choice of the tracking algorithm. In TempestExtremes (grid point detection of TC) the difference between LR and HR is larger than in TRACK (identification of relative vorticity after spectral filtering at truncation T63). The fact that the distribution of precipitation associated with all tropical vortices (i.e. when we relax the duration and warm core criteria) is less sensitive to resolution,

indicates that another type of convective systems compensates for the lack of precipitation in LR. In conclusion, we believe that the difference between LR and HR for low TCP5º can be attributed to tropical vortices not passing the threshold of TC identification.

(3) High TCP5º has little sensitivity to model resolution. This is the result of a large-scale balance.

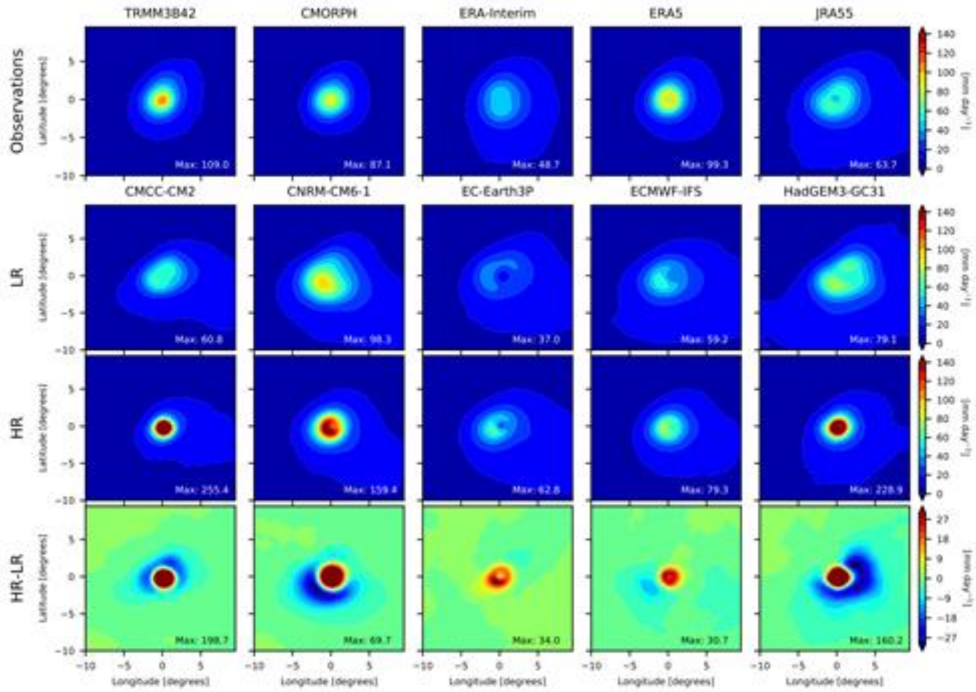

Figure T23.8: *composited precipitation for the 200 strongest tropical cyclones in each model over the period 1998-2014. Precipitation has been averaged over the full lifetime of all the storms. The composites are centred on MSLP. [1st row] observations and reanalysis [2nd row] LR, [3rd row] HR, [4th row] difference between HR and LR. Units are mm day^{-1}.*

Extratropical transition of North Atlantic tropical cyclones

Globally, approximately half of all tropical cyclones undergo extratropical transition and may, if landfalling, expose populous midlatitude regions to hurricane-force wind speeds and extreme precipitation. The frequency of tropical-origin storms across the North Atlantic is projected to increase this century (Haarsma et al., 2013), but a multi-model assessment based on PRIMAVERA simulations will help reduce projection uncertainties and inform assessments of present and future risk.

In PRIMAVERA, the structural evolution of each tracked tropical cyclone was examined by phase-space analysis of cyclone-relative thermal wind fields (Hart, 2003) to distinguish systems that retained axisymmetric, warm-core structures from those that underwent extratropical transition, acquiring frontal, cold-core structures. Considering only the transitioned tropical cyclones tracks, we computed track density and compared this field with reanalyses to evaluate the historical simulations. Over the North Atlantic, negative ensemble-mean biases (vs the mean track density field of seven reanalyses) in low-resolution models are reduced at high resolution in both highresSST-present and hist-1950 simulations (Fig. T23.9). Genesis density biases are also reduced at high-resolution (not shown).

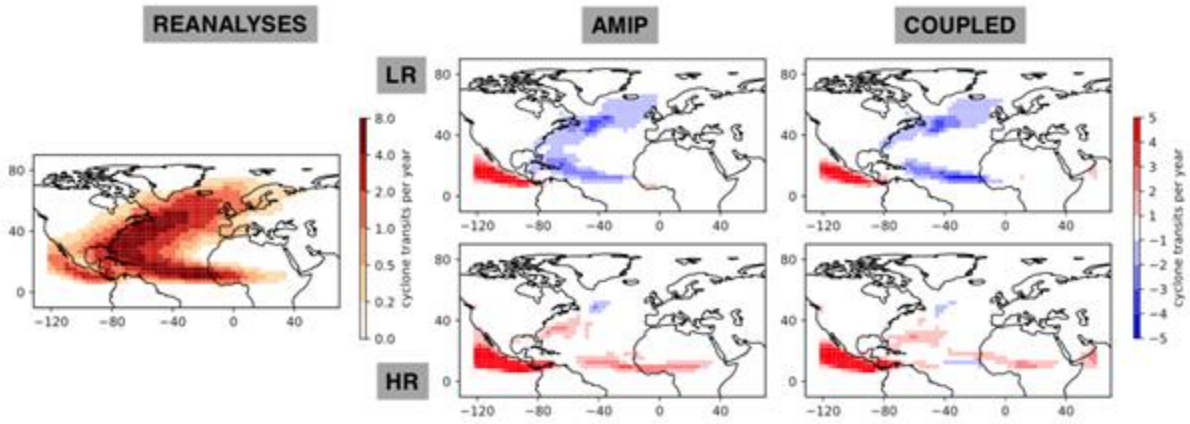

Figure T23.9: *Track density of tropical cyclones undergoing extratropical transition in reanalyses (left) and track density biases in (middle) highresSST-present and (right) hist-1950 simulations at (top) low and (bottom) high resolution.*

3.4 References

Altman, J., Ukhvatkina, O. N., Omelko, A. M., Macek, M., Plener, T., Pejcha, V. et al. (2018) Poleward migration of the destructive effects of tropical cyclones during the 20th century. Proceedings of the National Academy of Sciences, 115(45), 11543–11548. https://doi.org/10.1073/pnas.1808979115

Baker, A. J. Hodges, K. I., Schiemann, R. and Vidale, P. L., 2020: Historical variability and lifecycles of North Atlantic midlatitude cyclones originating in the tropics. Under review, Journal of Geophysical Research: Atmospheres.

Bellucci, A., and Coauthors: Air-sea interactions over the Gulf Stream in an ensemble of HighResMIP present climate simulations. Clim. Dyn., submitted

Boé J., L. Terray, M.-P. Moine, S. Valcke, A. Bellucci, S. Drijfhout, R. Haarsma, K. Lohmann, D. Putrasahan, C. Roberts, M. Roberts, E. Scoccimarro, J. Seddon, R. Senan, K. Wyser: Past long-term summer warming over western Europe in new generation climate models: role of large-scale atmospheric circulation, in press in Environmental Research Letters, https://doi.org/10.1088/1748-9326/ab8a89

Bishop SP, Small RJ, Bryan FO, Tomas RA (2017) Scale dependence of mid-latitude air–sea interaction,J Clim, 30: 8207–8221, https://doi.org/10.1175/JCLI-D-17-0159.1.

Caian, M., Koenigk, T., Döscher, R. et al. An interannual link between Arctic sea-ice cover and the North Atlantic Oscillation. Clim Dyn 50, 423–441 (2018). https://doi.org/10.1007/s00382-017-3618-9

Caron, L-P, CG Jones and K Winger (2011) Impact of resolution and downscaling technique in simulating recent Atlantic tropical cyclone activity. Climate Dynamics, 5, 869-892. doi: 10.1007/s00382-010-0846-7.

Cherchi, A., Fogli, P. G., Lovato, T., Peano, D., Iovino, D., Gualdi, S., et al. (2019). Global mean climate and main patterns of variability in the CMCC-CM2 coupled model. *Journal of Advances in Modeling Earth Systems*, 11, 185– 209. https://doi.org/10.1029/2018MS001369

Docquier D, Grist JP, Roberts MJ, Roberts CD, Semmler T, Ponsoni, L et al. (2019) Impact of model resolution on Arctic sea ice and North Atlantic Ocean heat transport. Clim Dyn, 53(7): 4989–5017. https://doi.org/10.1007/s00382-019-04840y.

Gleixner, S., Keenlyside, N., Hodges, K., Tseng, W.-L., & Bengtsson, L. (2014). An inter-hemispheric comparison of the tropical storm response to global warming. Clim. Dyn., 42, 2147–2157. https://doi.org/10.1007/s00382-013-1914-6

Grist, J. P., S. A. Josey, A. L. New, M. Roberts, T. Koenigk, D. Iovino, 2018: Increasing Atlantic ocean heat transport in the latest generation coupled ocean-atmosphere models: The role of air-sea interaction. JGR-Oceans, accepted. https://doi.org/10.1029/2018JC014387.

Haarsma, R. J., Hazeleger, W., Severijns, C., De Vries, H., Sterl, A., Bintanja, R., ... & van den Brink, H. W. (2013). More hurricanes to hit western Europe due to global warming. *Geophysical Research Letters*, *40*(9), 1783-1788.

Haarsma, R. J., García-Serrano, J., Prodhomme, C., Bellprat, O., Davini, P., & Drijfhout, S. (2019). Sensitivity of winter North Atlantic-European climate to resolved atmosphere and ocean dynamics. *Scientific reports*, *9*(1), 1-8.

Haarsma, R. J., Selten, F. M., & Drijfhout, S. S. (2015). Decelerating Atlantic meridional overturning circulation main cause of future west European summer atmospheric circulation changes. *Environmental Research Letters*, *10*(9), 94007.

Hodges, K., A. Cobb, and P. L. Vidale, 2017: How well are tropical cyclones represented in reanalysis datasets? J. Climate, 30, 5243–5264, https://doi.org/10.1175/JCLI-D-16-0557.1.

Jackson, L.C.,·M. J. Roberts, H. T. Hewitt, D. Iovino, T. Koenigk, V. L. Meccia, C. D. Roberts, Y. Ruprich-Robert, R. A. Wood, 2019: Does ocean resolution affect the rate of AMOC weakening? Clim. Dyn., revised.

Juricke, S., Palmer, T. N., Zanna, L., Juricke, S., Palmer, T. N., & Zanna, L. (2017). Stochastic sub-grid scale ocean mixing: Impacts on low frequency variability. Journal of Climate, JCLI-D-16-0539.1. https://doi.org/10.1175/JCLI-D-16-0539.1

Juricke, S., & Jung, T. (2014). Influence of stochastic sea ice parametrization on climate and the role of atmosphere-sea ice-ocean interaction. Philosophical Transactions of the Royal Society A: Mathematical, Physical and Engineering Sciences, 372(2018). https://doi.org/10.1098/rsta.2013.0283

Juricke, S., Lemke, P., Timmermann, R., & Rackow, T. (2013). Effects of stochastic ice strength perturbation on arctic finite element sea ice modeling. Journal of Climate. https://doi.org/10.1175/JCLI-D-12-00388.1

Kantha, L. (2006): Time to replace the Sar-Simpson hurricane scale? Eos, Transactions American Geophysical Union, 87.1, 3-6.

Keeley, S.P.E., Sutton, R.T. and Shaffrey, L.C. (2012), The impact of North Atlantic sea surface temperature errors on the simulation of North Atlantic European region climate. Q.J.R. Meteorol. Soc., 138: 1774-1783. doi:10.1002/qj.1912

Klaver, R., Haarsma, R., Vidale, P. L., & Hazeleger, W. (2020). Effective resolution in high resolution global atmospheric models for climate studies. *Atmospheric Science Letters*, *21*(4), e952.

Knutson, T., Camargo, S. J., Chan, J. C. L., Emanuel, K., Ho, C.-H., Kossin, J., et al. (2019). Tropical Cyclones and Climate Change Assessment: Part II. Projected Response to Anthropogenic Warming. Bulletin of the American Meteorological Society. https://doi.org/10.1175/BAMS-D-18-0194.1

Kossin, J. P., Emanuel, K. A., & Camargo, S. J. (2016). Past and Projected Changes in Western North Pacific Tropical Cyclone Exposure. Journal of Climate, 29(16), 5725–5739. https://doi.org/10.1175/JCLI-D-16-0076.1

Kossin, J. P., Emanuel, K. A., & Vecchi, G. A. (2014). The poleward migration of the location of tropical cyclone maximum intensity. Nature, 509(7500), 349–352. https://doi.org/10.1038/nature13278

Lee, R.W., Woollings, T.J., Hoskins, B.J. et al. (2018) Impact of Gulf Stream SST biases on the global atmospheric circulation. Clim Dyn 51, 3369–3387. https://doi.org/10.1007/s00382-018-4083-9

Li, F., M. S. Lozier, G. Danabasoglu, N. P. Holliday, Y. Kwon, A. Romanou, S. G. Yeager, and R. Zhang, 2019: Local and Downstream Relationships between Labrador Sea Water Volume and North Atlantic Meridional Overturning Circulation Variability. J. Climate, 32, 3883–3898, https://doi.org/10.1175/JCLI-D-18-0735.1.

Mahendran, M. (1998): Cyclone intensity categories. Weather and forecasting, 13.3, 878-883.

Moreno-Chamarro, E., L.-P. Caron, P. Ortega, S. L. Tomas, M. J. Roberts, 2020: Is winter precipitation change over Europe underestimated in current climate projections? Nat. Clim. Cha., submitted.

Powell, M. D. & Reinhold, T. A. (2007): Tropical cyclone destructive potential by integrated kinetic energy. Bulletin of the American Meteorological Society, 88.4, 513-526.

Roberts MJ et al (2020) Sensitivity of the Atlantic Meridional Overturning Circulation to Model Resolution in CMIP6 HighResMIP Simulations and Implications for Future Changes. J Adv Model Earth Sys, https://doi.org/10.1029/2019MS002014.

Roberts, M., and Coauthors (2015) Tropical cyclones in the UPSCALE ensemble of high-resolution global climate models. J. Climate, 28, 574–596, https://doi.org/10.1175/JCLI-D-14-00131.1

Roberts, M. J., J. Camp, J. Seddon, P. L. Vidale, K. Hodges, B. Vanniere, J. Mecking, R. Haarsma, A. Bellucci, E. Scoccimarro, L.-P. Caron, F. Chauvin, L. Terray, S. Valcke, M.-P. Moine, D. Putrasahan, C. Roberts, R. Senan, C. Zarzycki, P. Ullrich, 2020a: Impact of model resolution on tropical cyclone simulation using the HighResMIP-PRIMAVERA multi-model ensemble. J. Climate, 33, 7. https://doi.org/10.1175/JCLI-D-19-0639.1

Roberts, MJ, J Camp, J Seddon, PL Vidale, K Hodges, B Vanniere, J Mecking, R Haarsma, A Bellucci, E Scoccimarro, L-P Caron et al. (2020b) Projected Future Changes in Tropical Cyclones using the CMIP6 HighResMIP Multi-model Ensemble. Geophys Res Lett. https://agupubs.onlinelibrary.wiley.com/doi/abs/10.1029/2020GL088662.

Schiemann, R., Athanasiadis, P., Barriopedro, D., Doblas-Reyes, F., Lohmann, K., Roberts, M. J., et al. (2020). The representation of Northern Hemisphere blocking in current global climate models. *Weather and Climate Dynamics,* accepted. https://doi.org/10.5194/wcd-2019-19

Scoccimarro, E, S Gualdi, A Bellucci, D Peano, A Cherchi, G A. Vecchi, A Navarra (2020): The typhoon-induced drying of the Maritime Continent. Proceedings of the National Academy of Sciences, 117 (8) 3983-3988; DOI: 10.1073/pnas.1915364117

Scoccimarro, E., P.G. Fogli, K.A. Reed, S. Gualdi, S. Masina, and A. Navarra (2017): Tropical Cyclone Interaction with the Ocean: The Role of High-Frequency (Subdaily) Coupled Processes. J. Climate, 30, 145–162, https://doi.org/10.1175/JCLI-D-16-0292.1

Sharmila, S., & Walsh, K. J. E. (2018). Recent poleward shift of tropical cyclone formation linked to Hadley cell expansion. Nature Climate Change, 8(8), 730–736. https://doi.org/10.1038/s41558-018-0227-5

Strachan, J et al. (2013) Investigating Global Tropical Cyclone Activity with a Hierarchy of AGCMs: The Role of Model Resolution. J Clim, 26, 133-152.

Strong, C., Magnusdottir, G. Dependence of NAO variability on coupling with sea ice. Clim Dyn 36, 1681–1689 (2011). https://doi.org/10.1007/s00382-010-0752-z

Tsartsali, E.I and co-authors. Impact of resolution on atmosphere-ocean VMM and PAM coupling along the Gulf stream in global high resolution models. In preparation.

Ullrich, P. A., and C. M. Zarzycki, 2017: TempestExtremes: A framework for scale-insensitive pointwise feature tracking on unstructured grids. Geosci. Model Dev., 10, 1069–1090, https://doi.org/10.5194/gmd-10-1069-2017

Vanniere, B, M Roberts, PL Vidale, K Hodges, ME Demory, L-P Caron et al. (2020) The moisture budget of tropical cyclones: large scale environmental constraints and sensitivity to model horizontal resolution. J Climate. Accepted.

Vecchi GA, Delworth TL, Murakami H, Underwood SD, Wittenberg AT, Zeng F, Zhang W, Baldwin JW, Bhatia KT, Cooke W et al. (2019) Tropical cyclone sensitivities to CO2 doubling: roles of atmospheric resolution, synoptic variability and background climate changes. Climate Dynamics. 53, 5999–6033

Wang, L., Ting, M. & Kushner, P.J. A robust empirical seasonal prediction of winter NAO and surface climate. Sci Rep 7, 279 (2017). https://doi.org/10.1038/s41598-017-00353-y

Wehner, M. F., and Coauthors (2014) The effect of horizontal resolution on simulation quality in the Community Atmospheric Model, CAM5.1. J. Adv. Model. Earth Syst., 6, 980–997, https://doi.org/10.1002/2013MS000276.

Wu R, Kirtman B, Pegion K (2006) Local air–sea relationship in observations and model simulations, J Clim, 19:4914–4932, doi:10.1175/JCLI3904.1

Woollings, T., Hannachi, A. and Hoskins, B. (2010), Variability of the North Atlantic eddy-driven jet stream. Q.J.R. Meteorol. Soc., 136: 856-868. doi:10.1002/qj.625

Woollings, T., Barriopedro, D., Methven, J., Son, S.-W., Martius, O., Harvey, B., et al. (2018). Blocking and its Response to Climate Change. *Current Climate Change Reports*, 287–300. https://doi.org/10.1007/s40641-018-0108-z

Zhai, A. R. & Jiang, J. H. (2014): Dependence of US hurricane economic loss on maximum wind speed and storm size. Environmental Research Letters, 9.6

Zehnder, J. A., Powell, D. M. and Ropp, D. L. (1999) The interaction of easterly waves, orography and the intertropical convergence zone in the genesis of eastern Pacific tropical cyclones. Mon. Wea. Rev. 127, 1566–1585.

3.4 Peer reviewed articles supported by PRIMAVERA

Baker, A. J. Hodges, K. I., Schiemann, R. and Vidale, P. L., 2020: Historical variability and lifecycles of North Atlantic midlatitude cyclones originating in the tropics. Under review, Journal of Geophysical Research: Atmospheres

Boé J., L. Terray, M.-P. Moine, S. Valcke, A. Bellucci, S. Drijfhout, R. Haarsma, K. Lohmann, D. Putrasahan, C. Roberts, M. Roberts, E. Scoccimarro, J. Seddon, R. Senan, K. Wyser: Past long-term summer warming over western Europe in new generation climate models: role of large-scale atmospheric circulation, in press in Environmental Research Letters, https://doi.org/10.1088/1748-9326/ab8a89

Docquier D, Grist JP, Roberts MJ, Roberts CD, Semmler T, Ponsoni, L et al. (2019) Impact of model resolution on Arctic sea ice and North Atlantic Ocean heat transport. Clim Dyn, 53(7): 4989–5017. https://doi.org/10.1007/s00382-019-04840y.

Cherchi, A., Fogli, P. G., Lovato, T., Peano, D., Iovino, D., Gualdi, S., et al. (2019). Global mean climate and main patterns of variability in the CMCC-CM2 coupled model. *Journal of Advances in Modeling Earth Systems*, 11, 185– 209. https://doi.org/10.1029/2018MS001369

Grist, J. P., S. A. Josey, A. L. New, M. Roberts, T. Koenigk, D. Iovino, 2018: Increasing Atlantic ocean heat transport in the latest generation coupled ocean-atmosphere models: The role of air-sea interaction. JGR-Oceans, accepted. https://doi.org/10.1029/2018JC014387

Jackson, L.C.,·M. J. Roberts, H. T. Hewitt, D. Iovino, T. Koenigk, V. L. Meccia, C. D. Roberts, Y. Ruprich-Robert, R. A. Wood, 2019: Does ocean resolution affect the rate of AMOC weakening? Clim. Dyn., revised.

Haarsma, R. J., García-Serrano, J., Prodhomme, C., Bellprat, O., Davini, P., & Drijfhout, S. (2019). Sensitivity of winter North Atlantic-European climate to resolved atmosphere and ocean dynamics. *Scientific reports*, *9*(1), 1-8.

Klaver, R., Haarsma, R., Vidale, P. L., & Hazeleger, W. (2020). Effective resolution in high resolution global atmospheric models for climate studies. *Atmospheric Science Letters*, *21*(4), e952.

Kreussler, P. (2020) Change in tropical cyclone integrated kinetic energy between present and future climate in the cnrm climate model. *Master Thesis*.

Roberts MJ et al (2020) Sensitivity of the Atlantic Meridional Overturning Circulation to Model Resolution in CMIP6 HighResMIP Simulations and Implications for Future Changes. J Adv Model Earth Sys, https://doi.org/10.1029/2019MS002014.

Roberts, M. J., J. Camp, J. Seddon, P. L. Vidale, K. Hodges, B. Vanniere, J. Mecking, R. Haarsma, A. Bellucci, E. Scoccimarro, L.-P. Caron, F. Chauvin, L. Terray, S. Valcke, M.-P. Moine, D. Putrasahan, C. Roberts, R. Senan, C. Zarzycki, P. Ullrich, 2020: Impact of model resolution on tropical cyclone simulation using the HighResMIP-PRIMAVERA multi-model ensemble. J. Climate, 33, 7. https://doi.org/10.1175/JCLI-D-19-0639.1

Roberts, MJ, J Camp, J Seddon, PL Vidale, K Hodges, B Vanniere, J Mecking, R Haarsma, A Bellucci, E Scoccimarro, L-P Caron et al. (2020b) Projected Future Changes in Tropical Cyclones using the CMIP6 HighResMIP Multi-model Ensemble.

Geophys Res Lett. https://agupubs.onlinelibrary.wiley.com/doi/abs/10.1029/2020GL088662.

Schiemann, R., Athanasiadis, P., Barriopedro, D., Doblas-Reyes, F., Lohmann, K., Roberts, M. J., et al. (2020). The representation of Northern Hemisphere blocking in current global climate models. *Weather and Climate Dynamics,* accepted. https://doi.org/10.5194/wcd-2019-19

Scoccimarro, E, S Gualdi, A Bellucci, D Peano, A Cherchi, G A. Vecchi, A Navarra (2020): The typhoon-induced drying of the Maritime Continent. Proceedings of the National Academy of Sciences, 117 (8) 3983-3988; DOI: 10.1073/pnas.1915364117

Scoccimarro, E., P.G. Fogli, K.A. Reed, S. Gualdi, S. Masina, and A. Navarra (2017): Tropical Cyclone Interaction with the Ocean: The Role of High-Frequency (Subdaily) Coupled Processes. J. Climate, 30, 145–162, https://doi.org/10.1175/JCLI-D-16-0292.1

Tsartsali, E.l and co-authors. Impact of resolution on atmosphere-ocean VMM and PAM coupling along the Gulf stream in global high resolution models. In preparation.

Vanniere, B, M Roberts, PL Vidale, K Hodges, ME Demory, L-P Caron et al. (2020) The moisture budget of tropical cyclones: large scale environmental constraints and sensitivity to model horizontal resolution. J Climate. Accepted.

4. Lessons Learnt

The lessons learnt from Tasks 2.1-3 are that indeed enhancing ocean and atmosphere resolution affects positively the representation of specific atmospheric and oceanic processes. For some of these processes clear minimal requirements for resolution can be identified, but for other processes this is more of a gradual scale. On the other hand, many biases are related to parametrization errors and cannot be solved by enhancing resolution.

The use of HighResMIP protocol enabled for the first time to evaluate in a systematic way the impact of resolution. This initiative of a coherent protocol with many participating models, should be carried forward in the future, possibly with a new design of the protocol in agreement with new developments of computing facilities and model development. The design of such a new protocol should take into account the results obtained from HighResMIP.

Analysing the data on a central, common platform (JASMIN) was key to the success of the analyses. This was the only way to deal with the huge amount of data with high resolution simulations.

The development of the new high-resolution models, the simulations and the post-processing of the data took much more time than was initially foreseen. Even with the extension of nine months of the PRIMAVERA project, the time for analyses was short and there is much more analyses to be done on the HighResMIP data, as can be seen by the number of articles in prep., submitted or accepted during the last year of the project. It is expected that HighResMIP data will be a source of new research that will build on the results obtained so far in HighResMIP, of which many will find their way into the IPCC, WGI AR6 report.

It is useful if one person/group can generate some post-processed data in a consistent way for others to analyse, so reducing duplication of work. Examples include the tropical cyclone tracks and the AMOC analyses at 26.5°N consistent with observations. In the future, it would be great if the models could produce such standard datasets automatically, rather than having to push many 10’s TB of data through further algorithms.

The HighResMIP protocol did not specifically provide a separation between atmosphere and ocean resolution, however, the available simulations and analyses suggest that some processes benefit from an increase in ocean or atmosphere, whereas others require an increase in both components.

5. Links Built

Links have been built with WP1, 4, 5, 6, 10, and 11. Many of the diagnostics shown in this report are made through the use of ESMValTool developed in WP1. There are links created with other projects like CRESCENDO, ISIMIP. By sharing some analysis tools with international colleagues (e.g. Japanese groups, iHESP project), we were able to include additional models in some of the multi-model analysis. A strong link with IPCC has been created.